Estimates of *E. histolytica* infections have been based primarily on examinations of stool for cysts and parasites, but these tests are insensitive and cannot differentiate *E. histolytica* from morphologically identical species that are nonpathogenic, such as *E. dispar* and *Entamoeba moshkovskii*.[5,22] Specific and sensitive means to detect *E. histolytica* in stool are now available and include antigen detection and polymerase chain reaction (PCR).[34,41,56]

A prospective study of preschool children in a slum of Dhaka, Bangladesh, showed *E. histolytica*–associated diarrhea in 9 percent and *E. histolytica*–associated dysentery in 3 percent of the children annually.[39] Not all individuals are equally susceptible to amebiasis, with certain HLA-DR and HLA-DQ alleles associated with resistance to infection and disease.[23] The annual incidence of amebic liver abscess was reported to be 21 cases per 100,000 inhabitants in Hue City, Vietnam.[14] Carefully conducted serologic studies in Mexico, where amebiasis is endemic, showed antibody to *E. histolytica* in 8.4 percent of the population.[17] In the urban slum of Fortaleza, Brazil, 25 percent of all individuals tested carried antibody to *E. histolytica*; the prevalence of antiamebic antibodies in children 6 to 14 years old was 40 percent.[15]

PATHOGENESIS AND PATHOLOGY

The cysts are transported through the digestive tract to the intestine, where they release their mobile, disease-producing form, the trophozoite. *E. histolytica* trophozoites can live in the large intestine and form new cysts without causing disease. They also can invade the lining of the colon, killing host cells and causing diarrhea, amebic colitis, acute dysentery, or chronic diarrhea. The trophozoites also can be carried through the blood to other organs, most commonly the liver and occasionally the brain, where they form potentially life-threatening abscesses (Fig. 221–1). Important virulence factors include the trophozoite cell surface galactose and *N*-acetyl-D-galactosamine (Gal/GalNAc)–specific lectin that mediates adherence to colonic mucins and host cells,[74,86] cysteine proteinases that likely promote invasion by degrading extracellular matrix and serum components, and amoebapore pore-forming proteins involved in killing of bacteria and host cells.[57,88]

The interface of the Gal/GalNAc lectin with the host mucins lining the intestine is the defining moment of the infection.[19] If the parasite lectin attaches to the host mucin glycoproteins that line the intestinal lumen, a noninvasive gut infection ensues. The life cycle continues as the trophozoites reproduce by clonal expansion in the mucin layer. Subsequently, the Gal/GalNAc lectin, along with mucin glycoproteins or other gut bacteria, initiates the developmental pathway leading to encystment.[25,92]

Colitis is caused when the trophozoite penetrates the intestinal mucous layer, which otherwise acts as a barrier to invasion by inhibiting amebic adherence to the underlying epithelium and by slowing trophozoite motility.[19] Invasion is mediated by the killing of epithelial cells, neutrophils, and lymphocytes by trophozoites, which occurs only after the parasite lectin engages host GalNAc on O-linked cell surface oligosaccharides.[75] The interaction of the lectin with glycoconjugates is stereospecific and multivalent.[100] The identity of the high-affinity intestinal epithelial cell receptor is unknown. Secretion of amoebapore, a 5-kd pore-forming protein, by the ameba may contribute to killing.[55] Activation of human caspase 3, a distal effector molecule in the apoptotic pathway, occurs rapidly after amebic contact, and caspases are required for cell killing in vitro and for the formation of amebic liver abscesses in vivo.[45,90]

Interaction of the parasite with the intestinal epithelium causes an inflammatory response marked by the activation of nuclear factor κB and the secretion of cytokines.[24,89] The development of this epithelial response may depend on trophozoite virulence factors, such as cysteine proteinase, and leads to intestinal abnormalities through neutrophil-mediated damage. Neutrophils also can be protective, and activation of neutrophils or macrophages by tumor necrosis factor-α or interferon-γ kills amebae in vitro and limits the size of amebic liver abscesses.[7,21] In contrast to the intense inflammatory response, typical of early invasive amebiasis, inflammation surrounding well-established colonic ulcers and liver abscesses is minimal, given the degree of tissue damage.[16]

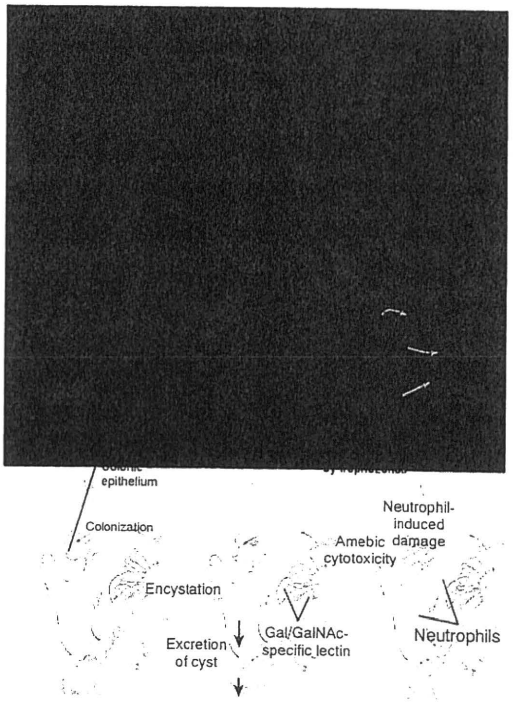

Figure 221–1 Life cycle of *Entamoeba histolytica*. Infection normally is initiated by the ingestion of fecally contaminated water or food containing *E. histolytica* cysts. The infective cyst form of the parasite survives passage through the stomach and small intestine. Excystation occurs in the bowel lumen, where motile and potentially invasive trophozoites are formed. In most infections, the trophozoites aggregate in the intestinal mucin layer and form new cysts, resulting in a self-limited and asymptomatic infection. In some cases, adherence to and lysis of the colonic epithelium, mediated by the galactose and *N*-acetyl-D-galactosamine (Gal/GalNAc)–specific lectin, initiates invasion of the colon by trophozoites. Neutrophils responding to the invasion contribute to cellular damage at the site of invasion. When the intestinal epithelium is invaded, extraintestinal spread to the peritoneum, liver, and other sites may follow. Factors controlling invasion, as opposed to encystation, most likely include parasite "quorum sensing" signaled by the Gal/GalNAc-specific lectin, interactions of amebae with the bacterial flora of the intestine, and innate and acquired immune responses of the host. (See companion Expert Consult web site for color version.) *(From Haque, R., Huston, C. D., Hughes, E., et al.: Amebiasis. N. Engl. J. Med. 348:1565-1573.)*

The initial lesions of clinical amebiasis often are small interglandular ulcers with a diameter of approximately 1 mm. They extend only to the muscularis mucosa.[16,64] The margins may be hyperemic, and slight edema of the surrounding mucosa is present. *E. histolytica* organisms seen in these ulcers stain well with periodic acid–Schiff stain.[76] Bleeding and friability are not prominent at this stage, although proctoscopic examination may find mucus coming from these ulcers, with an abundant number of amebae present.

The next stage of intestinal disease is the production of deeper ulcers. These "buttonhole" ulcers may be 1 cm in diameter and may extend into the submucosa.[16,76] The ulcer often extends laterally under normal-appearing mucosa, forming a characteristic flask shape. Occasional perforation through the serosa leads to peritonitis or pneumoperitoneum.[91] Extensive necrosis may be present, but usually only very little inflammation occurs. The edema is more intense, but the mucosa between ulcers is normal, in contrast to the marked inflammatory response seen in bacterial enteritis. When ulceration is more extensive, the edema surrounding the ulcers becomes confluent, and the mucosa appears gelatinous. In young children, this condition can progress to a fulminant necrotizing colitis associated with transmural necrosis. The pathologic events associated with this phenomenon are not understood. Rarely, an inflammatory response is present, resulting in granulation of the tissue with a fibrous outer wall.[72] It is given the name *ameboma*. Occasionally, an ameboma fills a significant portion of the lumen, which causes stricture or obstruction. Other complications of intestinal amebiasis result from direct extension of the ulcers. This extension may result in cutaneous involvement of the perianal area or lesions of the penis, vulva, vagina, or cervix.[2,72] Cutaneous and ophthalmologic amebiasis also is caused by fecal contamination of the face.[67]

Amebas disseminate to the liver in 50 percent of patients with fulminant amebiasis.[2,3] Dissemination to other organs directly from the intestine probably does not occur, but dissemination from the liver to lung, heart, brain, spleen, scapula, larynx, stomach, and aorta has been described.[16] Amebic abscess of the liver occurs more often in men than in women by a ratio of 16:1, but occurs equally often in prepubertal children of both sexes.[3,16] Abscesses occur more commonly in adults, but occur in children as young as 4 months of age.[70] These abscesses vary from microscopic lesions to massive necrosis of 90 percent of the liver. Fever, right upper quadrant pain, and the presence of serum antibodies to amebae point to hepatic amebic abscess.[84] Examination of the fluid from such an abscess frequently reveals a reddish, "anchovy paste" fluid that rarely may appear white or green. The fluid is acidic, with a pH ranging from 5.2 to 6.7.[82] Amebas are found in the walls of the abscess and only rarely in the fluid of the abscess. Many patients with amebic liver abscess also have anaerobic bacteria in the abscess fluid.[83] The walls are composed of a thin connective tissue capsule. The right lobe of the liver is involved with amebic liver abscess about six times as often as the left lobe. Abscesses in the right lobe can perforate and cause disease below the diaphragm or in the thoracic cavity. Abscesses in the left lobe can lead to pericardial effusions, which are less common than pleural effusions.[32,47]

Pleural effusions can remain loculated or lead to cutaneous fistulas or to bronchopleural fistulas. Drainage from these fistulas is acidic, in contrast to the neutral secretions in the normal lung. Seeding of the cardiac valves and of the brain has been described.[16] Cerebral abscesses have the same microscopic findings as do liver abscesses, with a thin capsule of connective tissue surrounding a fluid with little or no associated inflammatory response.

IMMUNITY

Protection from amebiasis, including acquired immunity to infection and invasion by *E. histolytica*, is associated with a mucosal IgA antibody response against the carbohydrate recognition domain of the parasite Gal/GalNAc lectin.[37,35,43,53] Cell-mediated immunity in protection from invasive amebiasis, but not infection per se, also has been shown. There is substantial evidence from in vitro, animal model, and most recently human studies of an important role for interferon-γ in protection from amebic colitis, acting in part by activating of macrophages to kill the parasite.[40,44] Invasive amebiasis rarely occurs in individuals with human immunodeficiency virus/acquired immunodeficiency syndrome, even in areas where amebiasis is common, suggesting an important role also exists for natural immunity or innate immune responses, or both, in protection from infection.[7,34]

CLINICAL MANIFESTATIONS

INTESTINAL AMEBIASIS

Asymptomatic Intraluminal Amebiasis

The most common type of amebic infestation is an asymptomatic cyst-passing carrier state. All *E. dispar* infections and 90 percent of *E. histolytica* infections are asymptomatic, manifesting with only *Entamoeba* cysts in the feces.[29,78] Some investigators have suggested that stools of these individuals generally are more liquid than stools of individuals without trophozoites.[26]

Entamoeba histolytica–Associated Diarrhea

Diarrhea is the most common manifestation of amebic disease, present in 9 percent of children in the Mirpur cohort each year, compared with only 3 percent of children having amebic colitis each year.[39] *E. histolytica*–associated diarrhea is defined as three or more unformed stools in a 24-hour period accompanied by a new episode of *E. histolytica* infection. This definition was validated previously in the cohort by (1) showing that diarrhea was approximately five times more common in the setting of a new infection (age-adjusted odds ratio for the association of new *E. histolytica* infection with diarrhea of 4.7; 95% confidence interval 2.9 to 7.6), and (2) showing by a complete bacteriologic, virologic, and parasitic work-up that only 32 percent of *E. histolytica*–associated diarrhea cases were co-infected with another pathogen compared with identification of an enteropathogen in 59 percent of all cases of diarrhea.[37]

Acute Amebic Colitis

Amebic dysentery was defined as a diarrheal stool sample containing occult or gross blood that was positive for *E. histolytica* antigen. Seventy percent of patients have a gradual onset of symptoms over 3 or 4 weeks after infestation, with increasingly severe diarrhea as the primary complaint, accompanied by general abdominal tenderness. Occasionally, the onset may be acute or may be delayed for several months after infestation. This onset differs from bacterial causes of dysentery, in which patients usually have only symptoms of 1 to 2 days' duration. The diarrhea is usually associated with pain in children. Pain may be of such severity that an acute abdomen is suspected.[2,10,48,76] The stools contain blood and mucus in virtually all cases.[2,76,77] Fever is present in only a few patients with amebic colitis. Abdominal distention and dehydration occur in less than 10 percent of patients. In young children, intussusception, perforation, peritonitis, or necrotizing colitis may develop rapidly.[10,48,91]

Ameboma

Unusual manifestations of amebic colitis include toxic megacolon (0.5% of cases, usually requires surgical intervention), ameboma (granulation tissue in colonic lumen mimicking colonic cancer in appearance), and a chronic nondysenteric form of infection that can manifest as years of waxing and waning diarrhea, abdominal pain, and weight loss (easily misdiagnosed as inflammatory bowel disease).

EXTRAINTESTINAL AMEBIASIS

Amebic Liver Abscess

The typical patient with an amebic liver abscess in the United States is an immigrant, usually a Hispanic/Asian/Pacific Islander; male; 20 to 40 years old; who presents with fever, right upper quadrant pain, leukocytosis, abnormal serum transaminases and alkaline phosphatase, and a defect on hepatic imaging study. Roughly 90 percent of patients with liver abscess are men. The abscess usually is single and is in the right lobe of the liver 80 percent of the time.[49] Most frequently, patients present with liver abscess without concurrent colitis. Amebae are seen infrequently in the stool at the time of diagnosis of liver abscess.[3] Liver abscess can manifest acutely with fever and right upper abdominal tenderness and pain, or subacutely, with prominent weight loss and less frequent fever and abdominal pain. The peripheral white blood cell count is elevated, as is the alkaline phosphatase level, in many patients.

Early evaluation of the hepatobiliary system with ultrasound or computed tomography (CT) is essential to show the abscess in the liver. The differential diagnosis of the lesion in the liver includes pyogenic abscess, hepatoma, and echinococcal cyst. Aspiration of the abscess occasionally is required to diagnose amebiasis (although amebae are visualized in the pus in only a few cases; if the abscess is pyogenic, the responsible bacteria are seen or cultured). Antibodies to *E. histolytica* are present in the serum of 92 to 97 percent of patients on acute presentation with amebic liver abscess and are very useful diagnostically. Unusual extraintestinal manifestations of amebiasis include direct extension of the liver abscess to pleura or pericardium and brain abscess. In a patient who presents with right upper quadrant pain, ultrasound, CT, or magnetic resonance imaging (MRI) should be performed to examine the liver and gallbladder.

If a space-filling defect in the liver is observed, the differential diagnosis includes (1) amebiasis (most common in men with a history of travel or residence in a developing country); (2) pyogenic or bacterial abscess (suspect in women, patients with cholecystitis, elderly individuals, individuals with diabetes, and patients presenting with jaundice); (3) echinococcal abscess (an incidental finding because echinococcal abscess should not cause pain or fever); and (4) cancer. Most patients with amebic liver abscess have detectable circulating antigen in serum and serum anti-amebic antibodies.[34]

In children, abdominal pain is reported infrequently with amebic liver abscess.[33,68] More commonly, high fever, abdominal distention, irritability, and tachypnea are noted. Some children are admitted to the hospital with a fever of unknown origin. Hepatomegaly occurs frequently, but elicitation of hepatic tenderness is not well documented. In one report, four of five children younger than 5 years died with amebic liver abscesses because the diagnosis was not suspected.[54] Death usually results from rupture of the liver abscess into the peritoneum, thorax, or pericardium, but may follow extensive hepatic damage and liver failure.[3,81]

Metastatic Amebiasis

Extra-abdominal amebiasis presumably follows direct extension from liver abscesses, rather than direct dissemination from the intestine.[3,16] Thoracic amebiasis is the most common type of extra-abdominal amebiasis and occurs in approximately 10 percent of patients with amebic liver abscess.[16,47] Symptoms depend on the type of involvement. Empyema, bronchohepatic fistulas, or extension of a pleuropulmonary abscess into the pericardium may occur.

Pericardial amebiasis is the next most common form of extraintestinal involvement and may result from rupture of a liver abscess in the left lobe of the liver into the pericardium or through extension of the right-sided pleural amebiasis.[16,27,28,32] It is estimated to occur in 3 percent of patients with hepatic abscesses.[28] It manifests as acute pericarditis with tamponade and, occasionally, as pneumopericardium.[27] Amebic liver abscess in the left lobe also may rupture directly into the left chest.[63]

Cerebral amebic abscesses were found in 8 percent of patients with amebic infections discovered at autopsy in one study.[58] In other studies, lower rates of 0.66 to 4.7 percent of patients with amebic liver abscess having brain abscesses were reported.[46] Patients with cerebral amebiasis frequently are so ill from the intestinal, liver, and possibly lung involvement that neurologic signs are not always assessed easily. In 18 patients with proven cerebral amebiasis, initial neurologic examination was normal in 13, and only 1 patient later developed seizures.

Other foci of infection are rare findings, but amebic rectovesical fistula formation and involvement of pharynx, heart, aorta, and scapula have been reported. Cutaneous extension after the adherence of perforated, inflamed bowel to the skin is an extremely painful and rare complication.[16,72] This situation also may arise after invasion of the skin by trophozoites emerging out from the rectum occurs.

DIAGNOSIS

A heightened suspicion of amebiasis should be present if the patient has been in a developing country as a resident or traveler. The diagnosis of amebiasis should be considered in any child who is passing diarrhea, bloody stools, or stools with mucus; any child with a hepatic abscess; and any febrile child with right upper quadrant pain, abdominal distention, or tachypnea.[34,68] In a patient with diarrhea, if blood is present in the stool (grossly bloody or occult blood positive), infectious (Shiga toxin–producing *E. coli*, *Salmonella*, *Shigella*, *Campylobacter*; and *E. histolytica*) and noninfectious (inflammatory bowel disease, diverticulosis, arteriovenous malformations, cancer) causes should be considered.

IMMUNOLOGIC OR MOLECULAR EXAMINATION OF STOOL OR SERA

E. histolytica infection was defined as a positive test for antigen in stool. Antigen was detected using the TechLab (Blacksburg, VA) *E. histolytica* II stool antigen detection test, which specifically detects *E. histolytica* and does not cross-react with *E. dispar* or *E. moshkovskii*. The antigen test is 95 percent sensitive and specific compared with the "gold standard" of *E. histolytica* culture and zymodeme determination. It also is 80 percent sensitive compared with real-time PCR for *E. histolytica* DNA in stool. Although real-time PCR is excellent in sensitivity and specificity, real-time PCR still is not practical for the measurement of infection in the thousands of stool samples analyzed in this prospective study, so we usually use the less sensitive but highly specific antigen detection test, recognizing that in doing so we may underestimate the incidence of amebiasis.[41,56] In addition, immunohistochemical staining of amebae is useful in a difficult-to-diagnose case. Serologic tests for anti-amebic antibodies also are a very useful tool in diagnosis, with sensitivity of 70 to 80 percent early in disease and approaching 100 percent sensitivity on convalescence. The combined use of serology and stool antigen detection test offers the best diagnostic approach.

MICROSCOPIC EXAMINATION OF STOOL

Before the development of new antigen detection and PCR tests, amebiasis was diagnosed by examining a stool sample through a microscope to determine whether *E. histolytica* cysts were present. This method often requires more than one specimen, however, because the number of cysts in the stool varies greatly. In addition, stool microscopy has limited sensitivity and specificity. The body's own immune system produces macrophage cells that can look like the amebae. Three different amebae—*E. histolytica*, which causes amebiasis, and *E. dispar* and *E. moshkovskii*, which do not cause disease—look identical under a microscope.[22]

NONINVASIVE DIAGNOSIS OF EXTRAINTESTINAL AMEBIASIS

Amebiasis outside the intestine has been even more difficult to diagnose. Clinical manifestations of extraintestinal disease vary widely, and less than 10 percent of individuals with amebic liver abscesses have identifiable *E. histolytica* in their stools. The TechLab *E. histolytica* II test, which differentiates the true pathogen *E. histolytica* from *E. dispar*, was reported to detect Gal/GalNAc lectin in the sera of 22 of 23 (96%) patients with amebic liver abscess tested before treatment with the anti-amebic drug metronidazole and 0 of 70 (0%) controls. After 1 week of treatment with metronidazole, more than 80 percent of patients became serum lectin antigen–negative. Detection of *E. histolytica* Gal/GalNAc lectin in the sera using the TechLab *E. histolytica* II kit is sensitive to diagnose hepatic and intestinal amebiasis before the institution of metronidazole treatment.[38]

Noninvasive diagnostic procedures such as ultrasound, CT, and MRI can detect extracolonic amebiasis in the liver, paracecal masses, brain, and other sites, but they cannot distinguish between abscesses caused by amebae and those caused by bacteria, hampering proper treatment of the condition. Most patients with amebic liver abscess have a single abscess in the right lobe of the liver, although multiple lesions also can occur.[4] Chest radiographs show elevation of the right diaphragm in 56 percent of patients with hepatic abscess.[3] The diagnosis of cerebral amebiasis requires careful neurologic evaluation and radiographic evaluation with either CT or MRI.[16,46,58] Because of the risk for perforation, barium studies are relatively contraindicated in patients with amebic colitis.

BIOPSY STUDIES

The colonic and rectal mucosa in amebic colitis usually reveals ulcerations with a diameter of 1 to 10 mm. Amebic trophozoites often are at the periphery of these necrotic areas, which can be sampled through a biopsy specimen taken during sigmoidoscopy or colonoscopy.[42,49] Because of the potential for perforation, colonoscopy should be undertaken with caution.

In patients with amebic liver abscesses, amebic trophozoites are found near the capsule of the abscess. Until more recently, the most accurate diagnostic test involved the examination of a sample collected from the abscess tissue by needle aspiration, a procedure that is painful, potentially dangerous, and relatively insensitive, identifying amebic trophozoites only 20 percent of the time.

DIFFERENTIAL DIAGNOSIS

Invasive amebic colitis may resemble ulcerative colitis, Crohn disease of the colon (inflammatory bowel disease), bacillary dysentery, or tuberculous colitis.[11,18,42,89] Stool examinations, colonoscopic examination with biopsies, and serologic examination should be able to differentiate amebic colitis from these diseases. Histologic examination of involved colonic mucosa should differentiate amebic colitis, with its lack of inflammation and rare granulation tissue, from the inflammatory responses seen in ulcerative colitis, bacillary dysentery, and Crohn disease of the colon. Tuberculous colitis and Crohn disease are more likely to show granuloma formation than amebiasis. Ileocecal or small bowel involvement as seen on barium studies would suggest Crohn disease or tuberculosis of the gastrointestinal tract, rather than amebiasis. Tuberculous colitis usually is associated with pulmonary tuberculosis and with a strong reaction to tuberculin skin testing. In some cases, differentiating between invasive amebic colitis and inflammatory bowel disease may be impossible. If a patient with this differential diagnosis is placed on corticosteroids and deteriorates, the corticosteroids should be stopped, and repeat investigation for amebiasis should be performed.[18,68,72]

Amebic liver abscess must be differentiated from pyogenic abscesses and neoplastic lesions. Detection of *E. histolytica* Gal/GalNAc lectin in the sera using the TechLab *E. histolytica* II kit is quite helpful to diagnose hepatic and intestinal amebiasis before the institution of metronidazole treatment.[38] Total leukocyte counts and cultures of blood may help to differentiate pyogenic and amebic abscesses. Many children with pyogenic liver abscesses have negative blood cultures, however. Often, amebic and pyogenic liver abscesses show similar features on CT and MRI. Occasionally, nuclear imaging with gallium is helpful because, in contrast to a pyogenic abscess, very few neutrophils are contained within an amebic liver abscess.[85,87] Gallium scanning of an amebic liver abscess may reveal a cold spot, possibly with a bright rim. Several investigators recommend a trial using an appropriate drug for amebic abscess for 3 or 4 days while serologic and culture results are awaited.[68,98] Patients with amebic liver abscess should respond to treatment in this length of time by becoming afebrile. No change in size of the liver or size of the abscess should be noted at this time because resolution of the abscess usually takes 2 months to several years.[4,79,80,90,97]

COMPLICATIONS

Complications of amebiasis may be prevented by early establishment of diagnosis and initiation of treatment with appropriate agents.[46,68] When complications occur, the prognosis generally is poor.

Invasive intestinal amebiasis has been associated most commonly with perforation and peritonitis,[8,10,48,68,91,96] which apparently are an end result of "necrotizing" or "toxic" amebic colitis. In children, perforation may be heralded by the appearance of an acute abdomen or pneumoperitoneum, with rapid progression to death, presumably from sepsis.[8,68,96] Surgical resection and therapy for endotoxic shock improve the prognosis.[96] This complication is not rare and accounts for more than 30 percent of deaths from amebiasis in children.[11,50] Massive intestinal hemorrhage causes approximately 3 percent of deaths from amebiasis. Intussusception occasionally occurs and can be reduced with gentle barium enema. Multiple colonic strictures also can occur and cause obstructive symptoms. Fistulas to other organs or to the skin may develop.

Liver abscesses and their resultant complications account for approximately 40 percent of deaths from amebiasis.[50] Liver abscess also was found in 13 percent of patients with amebiasis who had postmortem examinations. Liver abscess with rupture into the abdomen was present in 8 percent of patients who died with amebiasis, and rupture of a liver abscess into the right pleural space was found in 12 percent.[50] Many patients with amebic liver abscess also have anaerobic bacteria in the abscess fluid.[83] In cases free of bacterial contamination, the fluid has few

inflammatory cells and an acidic pH. Amebic pericarditis or pneumopericardium occurs rarely and is found in only 1 percent of patients whose deaths were caused by amebiasis.[27,28,32,50] The fluid is similar to that found in the pleural space. A cerebral abscess was found in 4 percent of patients with amebiasis who died.[50] It has been reported in fewer than 10 children, only one of whom survived.[9,16,56,58] Other complications include infections of the retroperitoneal space, stomach, spleen, esophagus, and duodenum.[58]

TREATMENT

INTESTINAL AMEBIASIS

Asymptomatic Intraluminal Amebiasis

Therapy for asymptomatic and noninvasive infection differs from therapy for invasive infection. Asymptomatic infections may be treated with intraluminal agents, such as paromomycin or diloxanide furoate. Each agent has a high rate of success for eradication of cyst passage.[65,66] Paromomycin is a nonabsorbable aminoglycoside that is active against the cyst and trophozoite stages. High cure rates have been reported with a 7-day oral dose of paromomycin at 25 to 35 mg/kg/day in three divided doses (Table 221–2). Diloxanide furoate (Furamide) is a poorly absorbed agent that is quite active against only intraluminal amebiasis, but treats symptomatic and asymptomatic disease.[62,98] Cure rates have been greater than 90 percent with a 10-day oral course of diloxanide furoate at 20 mg/kg/day in three divided doses (maximum dose of 1500 mg/day).[65,66,73]

Acute Amebic Colitis

Nitroimidazoles, particularly metronidazole, are the mainstay of therapy for invasive amebiasis.[37] The oral dosage of metronidazole is 35 to 50 mg/kg/day (to a maximum of 2250 mg/day) in three divided doses for 7 to 10 days for severe intestinal or extraintestinal amebiasis. Metronidazole is concentrated in the ameba, probably via reduction of its nitro group by ferredoxin or flavodoxin-like electron transport proteins, which maintain a gradient for the entry of the unchanged drug. Metabolic intermediates of metronidazole damage DNA and possibly other macromolecules, and they deprive the organism of reducing equivalents by acting as an electron sink. Nitroimidazoles with longer half-lives (tinidazole, secnidazole, and ornidazole) are better tolerated and allow shorter periods of treatment.[38] The oral dosage of tinidazole is 60 mg/kg/day (to a maximum of 2000 mg/day) for 5 days for severe intestinal or extraintestinal amebiasis (see Table 221–2) (see http://www.medletter.com/).

Approximately 90 percent of patients who present with mild-to-moderate amebic dysentery have a response to nitroimidazole therapy. In the rare case of fulminant amebic colitis, adding broad-spectrum antibiotics to treat intestinal bacteria that may spill into the peritoneum is prudent; surgical intervention occasionally is required for acute abdomen, gastrointestinal bleeding, or toxic megacolon.[37] Agents such as metronidazole that are active against invasive and extraintestinal amebiasis are well absorbed and do not stay in the lumen long enough to have an effect on intestinal amebiasis. Parasites persist in the intestine in 40 to 60 percent of patients who receive nitroimidazole. Nitroimidazole treatment should be followed with paromomycin or the second-line agent diloxanide furoate to cure luminal infection.[38] Metronidazole and paromomycin should not be given at the same time because the diarrhea that is a common side effect of paromomycin may render assessing the patient's response to therapy difficult.[50-52]

EXTRAINTESTINAL AMEBIASIS

Amebic Liver Abscess and Metastatic Amebiasis

Extraintestinal and severe intestinal amebiasis must be treated with the tissue-active agents. Metronidazole (35 to 50 mg/kg/day in three divided doses for 7 to 10 days) is the preferred drug because it is effective and relatively free of serious side effects (see Table 221–2).[2,3,62,85,87,98] It is effective for extraintestinal amebiasis in any location, although amebic brain abscesses usually are not treated successfully with any medications. Most patients with amebic liver abscess respond to metronidazole within 72 hours. For amebic colitis, follow-up therapy with a luminal agent is very important because of the high rates of asymptomatic intestinal colonization in patients with amebic liver abscess.

Therapeutic aspiration of an amebic liver abscess occasionally is required as an adjunct to antiparasitic therapy. Drainage of the abscess should be considered in patients who have no clinical response to drug therapy within 5 to 7 days or patients with a high risk of experiencing rupture of the abscess, as defined by a cavity with a diameter of more than 5 cm or by the presence of lesions in the left lobe.[95] Because many patients with amebic liver abscess also have anaerobic bacteria in the abscess fluid,[83] addition of antibiotics, drainage, or both to the treatment regimen in the absence of a prompt response to nitroimidazole therapy is reasonable. Imaging-guided percutaneous treatment (needle aspiration or catheter drainage) has replaced surgical intervention as the procedure of choice for reducing the size of an abscess.[95]

PROGNOSIS

Invasive disease develops in 50 million people each year, and 50,000 to 100,000 deaths per year are caused by the invasive disease.[78,84,85] The case-fatality ratio is between 1 in 500 and 1 in 1000 diagnosed cases. Among patients with illness severe enough to require hospitalization, the case-fatality ratio is higher. One small study in children reported a 9 percent mortality rate and a 27 percent morbidity rate.[98]

Bowel necrosis or perforation is the cause of death from purely intestinal amebiasis, and early surgical intervention can reduce the mortality rate of these complications from 100 to 28 percent.[96] Amebic liver abscess has a case-fatality rate of 10 to 15 percent in combined figures of adults and children.[54,70,81] The mortality rate when pleural involvement is noted is 14 percent.[47,54] Amebic pericarditis has a case-fatality rate of 40 percent.[32] Cerebral amebiasis has a case-fatality rate of 96 percent.

TABLE 221–2 Pediatric Dosage of Drugs for Amebiasis

Symptomatic	Paromomycin	25-35 mg/kg/day in 3 doses × 7 days
Mild-to-moderate intestinal disease	Metronidazole	35-50 mg/kg/day in 3 doses × 7-10 days
	Trinidazole	50 mg/kg (maximum 2000 mg) qd × 3 days
Severe intestinal and extraintestinal disease	Metronidazole	35-50 mg/kg/day in 3 doses × 7-10 days
	Trinidazole	60 mg/kg/day (maximum 2000 mg) × 5 days

FUTURE

In a perfect world, amebiasis would be prevented by eradicating fecal contamination of food and water. Providing safe food and water for all children in developing countries would require massive societal changes and monetary investments. An effective vaccine would be much less costly, and for several reasons, a vaccine is a desirable and feasible goal. The high incidence of amebiasis in more recent community-based studies suggests that an effective vaccine would improve child health in developing countries.

The fact that humans naturally acquire partial immunity against intestinal infection indicates that barriers to stimulating an effective acquired immune response should not be insurmountable. Aiding vaccine design is the demonstration that several recombinant antigens, including the Gal/GalNAc-specific lectin, provide protection in animal models of amebiasis, and that human immunity is linked to intestinal IgA against the lectin.[35,37,43] The high degree of sequence conservation of the Gal/GalNAc-specific lectin suggests that a vaccine could be broadly protective. Finally, the absence of epidemiologically significant animal reservoirs suggests that herd immunity could interrupt fecal-oral transmission in humans. The challenges will be to design vaccines capable of eliciting durable mucosal immunity, to understand the correlates of acquired immunity, and, most important, to enlist the continued support of industrialized nations to combat diarrheal diseases of children in developing countries.

REFERENCES

1. Abd-Alla, M., Wahib, A., and Ravdin, J. I.: Diagnosis of amoebic colitis by antigen capture ELISA in patients presenting with acute diarrhoea in Cairo, Egypt. Trop. Med. Int. Health 7:1-6, 2002.
2. Adams, E. B., and MacLeod, I. N.: Invasive amebiasis, I: Amebic dysentery and its complications. Medicine *56*:315-323, 1977.
3. Adams, E. B., and MacLeod, I. N.: Invasive amebiasis, II: Amebic liver abscess and its complications. Medicine *56*:325-334, 1977.
4. Ahmed, L., Salama, Z. A., El Rooby, A., et al.: Ultrasonographic resolution time for amebic liver abscess. Am. J. Trop. Med. Hyg. *41*:406-410, 1989.
5. Ali, I. K. M., Hossain, M. B., Roy, S., et al.: *Entamoeba moshkovskii* infections in children in Bangladesh. Emerg. Infect. Dis. *9*:580-584, 2003.
6. Ali, I. K. M., Mondal, D., Roy, S., et al.: Evidence for a link between parasite genotype and outcome of infection with *Entamoeba histolytica*. J. Clin. Microbiol. *45*:285-289, 2007.
7. Asgharpour, A., Gilchrist, C., Baba, D., et al.: Resistance to intestinal *Entamoeba histolytica* infection is conferred by innate immunity and Gr-1+ cells. Infect. Immun. *73*:4522-4529, 2005.
8. Azar, H., Nazarian, I., and Sadrieh, M.: A study of cause of death in patients with fulminant amebic colitis. Am. J. Proctol. *28*:80-84, 1977.
9. Bachy, A.: Cerebral abscesses in amebiasis. J. Pediatr. *88*:364-365, 1976.
10. Balikian, J. P., Bitar, J. G., Rishani, K. K., et al.: Fulminant necrotizing amebic colitis in children. Am. J. Proctol. *28*:69-73, 1977.
11. Balikian, J. P., Uthman, S. M., and Kabalian, H. A.: Tuberculous colitis. Am. J. Proctol. *28*:75-79, 1977.
12. Barker, D. C.: Differentiation of *Entamoeba*: Patterns of nucleic acids and ribosomes during encystation and excystation. *In* Van den Bossche, H. (ed.): Biochemistry of Parasites and Host-Parasite Relationships. Amsterdam, Elsevier Biomedical, 1976, p. 253.
13. Barwick, R., Uzicanin, A., Lareau, S., et al.: Outbreak of amebiasis in Tbilisi, Republic of Georgia, 1998. Am. J. Trop. Med. Hyg. *67*:623-631, 2002.
14. Blessmann, J., Van Linh, P., Nu, P. A., et al.: Epidemiology of amebiasis in a region of high incidence of amebic liver abscess in central Vietnam. Am. J. Trop. Med. Hyg. *66*:578-583, 2002.
15. Braga, L. L., Lima, A. A., Sears, C. L., et al.: Seroepidemiology of *Entamoeba histolytica* in a slum in northeastern Brazil. Am. J. Trop. Med. Hyg. *55*:693-697, 1996.
16. Brandt, H., and Tamayo, R. P.: Pathology of human amebiasis. Hum. Pathol. *1*:351-385, 1970.
17. Caballero-Salcedo, A., Viveros-Rogel, M., Salvatierra, B., et al.: Seroepidemiology of amebiasis in Mexico. Am. J. Trop. Med. Hyg. *50*:412-419, 1994.
18. Case records of the Massachusetts General Hospital: Weekly clinicopathological exercises: Case 32-1977. N. Engl. J. Med. *297*:322-330, 1977.
19. Chadee, K., Petri, W. A., Jr., Innes, D. J., et al.: Rat and human colonic mucins bind to and inhibit the adherence lectin of *Entamoeba histolytica*. J. Clin. Invest. *80*:1245-1254, 1987.
20. Councilman, W. T., and Lafleur, H. A.: Amoebic dysentery. Johns Hopkins Hosp. Rep. *2*:395-548, 1891.
21. Denis, M., and Chadee, K.: Human neutrophils activated by interferon-gamma and tumour necrosis factor-alpha kill *Entamoeba histolytica* trophozoites in vitro. J. Leukoc. Biol. *46*:270-274, 1989.
22. Diamond, L. S., and Clark, C. G.: A redescription of *Entamoeba histolytica* (Schaudinn, 1903) (Emended Walker, 1911) separating it from *Entamoeba dispar* (Brumpt, 1925). J. Eukaryot. Microbiol. *40*:340-344, 1993.
23. Duggal, P., Haque, R., Roy, S., et al.: Influence of human leukocyte antigen class II alleles on susceptibility to *Entamoeba histolytica* infection in Bangladeshi children. J. Infect. Dis. *189*:520-526, 2004.
24. Eckmann, L., Reed, S. L., Smith, J. R., et al.: *Entamoeba histolytica* trophozoites induce an inflammatory cytokine response by cultured human cells through the paracrine action of cytolytically released interleukin-1 alpha. J. Clin. Invest. *96*:1269-1279, 1995.
25. Eichinger, D.: A role for a galactose lectin and its ligands during encystment of *Entamoeba*. J. Eukarot. Microbiol. *48*:17-21, 2001.
26. Elsdon-Dew, R.: The epidemiology of amoebiasis. Adv. Parasitol. *6*:1-62, 1968.
27. Freeman, A. L., and Bhoola, K. D.: Pneumopericardium complicating amoebic liver abscess: A case report. S. Afr. Med. J. *50*:551-553, 1976.
28. Ganesan, T. K., and Kandaswamy, S.: Amebic pericarditis. Chest *67*:112-113, 1975.
29. Gathiram, V., and Jackson, T. F.: Frequency distribution of *Entamoeba histolytica* zymodemes in a rural South African population. Lancet *1*:719-721, 1985.
30. Gathiram, V., and Jackson, T. F.: A longitudinal study of asymptomatic carriers of pathogenic zymodemes of *Entamoeba histolytica*. S. Afr. Med. J. *72*:669-672, 1987.
31. Griffin, J. L.: Human amebic dysentery: Electron microscopy of *Entamoeba histolytica* contacting, ingesting, and digesting inflammatory cells. Am. J. Trop. Med. Hyg. *21*:895-906, 1972.
32. Guimaraes, A. C., Vinhaes, L. A., Filho, A. S., et al.: Acute suppurative amebic pericarditis. Am. J. Cardiol. *34*:103-106, 1974.
33. Haffar, A., Boland, J., and Edwards, M. S.: Amebic liver abscess in children. Pediatr. Infect. Dis. *1*:322-327, 1982.
34. Hamano, S., Asgharpour, A., Stroup, S. E., et al.: Resistance of C57BL/6 mice to amoebiasis is mediated by nonhemopoietic cells but requires hemopoietic IL-10 production. J. Immunol. *177*:1208-1213, 2006.
35. Haque, R., Ali, I. K. M., Sack, R. B., et al.: Amebiasis and mucosal IgA antibody against the *Entamoeba histolytica* adherence lectin in Bangladeshi children. J. Infect. Dis. *183*:1787-1793, 2001.
36. Haque, R., Duggal, P., Ali, I. K. M., et al.: Innate and acquired resistance to amebiasis in Bangladeshi children. J. Infect. Dis. *86*:547-552, 2002.
37. Haque, R., Huston, C. D., Hughes, M., et al.: Amebiasis. N. Engl. J. Med. *348*:1565-1573, 2003.
38. Haque, R., Mollah, N. U., Ali, I. K. M., et al.: Diagnosis of amebic liver abscess and intestinal infection with the TechLab *Entamoeba histolytica* II antigen detection and antibody tests. J. Clin. Microbiol. *38*:3235-3239, 2000.
39. Haque, R., Mondal, D., Duggal, P., et al.: *Entamoeba histolytica* infection in children and protection from subsequent amebiasis. Infect. Immun. *74*:904-909, 2006.
40. Haque, R., Mondal, D., Shu, J., et al.: Correlation of IFN-γ production by peripheral blood mononuclear cells with childhood malnutrition and susceptibility to amebiasis. Am. J. Trop. Med. Hyg. *76*:340-344, 2007.
41. Haque, R., Roy, S., Siddique, A., et al.: Multiplex real-time PCR assay for detection of *Entamoeba histolytica*, *Giardia lamblia* and *Cryptosporidium* spp. Am. J. Trop. Med. Hyg. *76*:713-717, 2007.
42. Harries, J.: Amoebiasis: A review. J. R. Soc. Med. *75*:190-197, 1982.
43. Houpt, E. R., Barroso, L., Lockhart, L., et al.: Prevention of intestinal amebiasis by vaccination with the *Entamoeba histolytica* Gal/GalNac lectin. Vaccine *22*:611-617, 2004.
44. Houpt, E. R., Glembocki, D. J., Obrig, T. G., et al.: The mouse model of amebic colitis reveals mouse strain susceptibility to infection and exacerbation of disease by CD4+ T cells. J. Immunol. *169*:4496-4503, 2002.
45. Huston, C. D., Houpt, E. R., Mann, B. J., et al.: Caspase 3-dependent killing of host cells by the parasite *Entamoeba histolytica*. Cell. Microbiol. *2*:617-625, 2000.
46. Huston, C. D., and Petri, W. A., Jr.: Host-pathogen interaction in amebiasis and progress in vaccine development. Eur. J. Clin. Microbiol. Infect. Dis. *17*:601-614, 1998.
47. Ibarra-Perez, C., and Selman-Lama, M.: Diagnosis and treatment of amebic "empyema": Report of eighty-eight cases. Am. J. Surg. *134*:283-287, 1977.
48. Kala, P. C., Sharma, G. C., and Haldia, K. N.: Fulminating amoebic colitis with multiple perforations. Am. J. Proctol. *28*:31-34, 1977.
49. Katzenstein, D., Rickerson, V., Braude, A., et al.: New concepts of amebic liver abscess derived from hepatic imaging, serodiagnosis, and hepatic enzymes in 67 consecutive cases in San Diego. Medicine (Baltimore) *61*:237-246, 1982.
50. Kean, B. H., Gilmore, H. R., Jr., and Van Stone, W. W.: Fatal amebiasis: Report of 148 fatal cases from the Armed Forces Institutes of Pathology. Ann. Intern. Med. *44*:831-843, 1956.

Cellular Microbiology (2009) **11**(10), 1471–1491

doi:10.1111/j.1462-5822.2009.01341.x
First published online 29 June 2009

Phosphatidylinositol-phosphates mediate cytoskeletal reorganization during phagocytosis via a unique modular protein consisting of RhoGEF/DH and FYVE domains in the parasitic protozoon *Entamoeba histolytica*

Kumiko Nakada-Tsukui, Hiroyuki Okada, Biswa Nath Mitra and Tomoyoshi Nozaki*
Department of Parasitology, National Institute of Infectious Diseases, 1-23-1 Toyama, Shinjuku-ku, Tokyo 162-8640, Japan.

Summary

To understand the roles of phosphoinositides [PtdIns] in phagocytosis of parasitic eukaryotes, we examined the interaction of phosphatidylinositol-3-phosphate [PtdIns(3)P] and putative PtdIns-P-binding proteins during phagocytosis in the enteric protozoan parasite *Entamoeba histolytica*. It was previously shown that phagocytosis in *E. histolytica* is indispensable for virulence and is inhibited by PtdIns 3-kinase inhibitors. We demonstrated by time-lapse live imaging that during the initiation of phagocytosis, the PtdIns(3)P biomarker GFP–Hrs–FYVE, was translocated to the phagocytic cup, phagosome, and to tunnel-like structures connecting the plasma membrane and phagosomes. *E. histolytica* possesses 12 FYVE domain-containing proteins (EhFP1-12), 11 of which also contain the RhoGEF/DH domain. Among them EhFP4 was shown to be recruited to the tunnel-like structures and to the proximal region of the phagosome. We further demonstrated that EhFP4 physically interacted with 4 of 10 predominant Rho/Rac small GTPases. Phosphoinositide binding assay showed that EhFP4 unexpectedly bound to PtdIns(4)P via the carboxyl-terminal domain and that the FYVE domain modulates the binding specificity of EhFP4 to PtdIns-P. Expression of the FYVE domain from EhFP4 inhibited phagocytosis while enhancement was observed when mammalian Hrs–FYVE domain was expressed. Altogether, we demonstrated that PtdIns(3)P, PtdIns(4)P and EhFP4 coordinately regulate phagocytosis and phagosome maturation in this parasitic eukaryote.

Received 10 March, 2009; revised 19 May, 2009; accepted 1 June, 2009. *For correspondence. E-mail: nozaki@nih.go.jp; Tel. (+81) 3 5285 1111 ext. 2600; Fax (+81) 3 5285 1219 or 1173.

Introduction

Entamoeba histolytica is a major cause of colitis and liver abscess in developing countries (Haque *et al.*, 2003; Ackers and Mirelman, 2006). Recently, several molecules playing fundamental roles in the biology and virulence of this parasite have been identified. Among them are the cell surface galactose/*N*-acetylgalactosamine-specific lectins, cysteine proteases and amoebapores, which are involved in the interaction with host cells and bacteria, the destruction of immune and non-immune cells, or in the digestion of ingested microorganisms respectively (Que and Reed, 2000; Frederick and Petri, 2005). In addition to these molecules, phagocytosis and motility have been shown to play a pivotal role in the establishment of infection (Labruyere and Guillen, 2006). It was demonstrated that phagocytosis and cell movement are controlled by the cytoskeleton and its regulators, including actins, myosins, p21 activated kinases and Rho/Rac small GTPases (Guillen *et al.*, 1998; Voigt and Guillen, 1999; Labruyere *et al.*, 2003; Coudrier *et al.*, 2005; Marion *et al.*, 2005; Arias-Romero *et al.*, 2006; Franco-Barraza *et al.*, 2006). Rho guanine nucleotide exchange factor (RhoGEF), the activator of Rho/Rac small GTPases, is also important in regulating biological processes where cytoskeletal reorganization is involved, including chemotaxis, cytokinesis, tumorigenesis and phagocytosis (Rossman *et al.*, 2005; Vargas and Gonzalez-de la Rosa, 2007). The number of RhoGEFs in the *E. histolytica* and human genomes are also comparable. Sixty-two RhoGEFs have been identified in *E. histolytica*, all belonging to the Dbl homology (DH) protein family, while 69 RhoGEFs are present in man (Vargas and Gonzalez-de la Rosa, 2007).

It should be emphasized that the molecular mechanisms of phagocytosis in *E. histolytica* are significantly divergent from well-established models found in other organisms, particularly to the professional phagocytes of mammals. First, among three main elements of the eukaryotic cytoskeleton, *E. histolytica* seems heavily dependent on actin microfilaments (Loftus *et al.*, 2005; Clark *et al.*, 2007). *E. histolytica* has a number of actin binding proteins to modify filamentous actins and highly conserved Arp2/3 complex, but lacks WASP/SCAR proteins, for actin nucleation by the Arp2/3 complex. Second, *E. histolytica* has only two myosins, myosin IB and myosin II, and lacks other myosins, like myosin V, that are considered ubiquitous (Labruyere and Guillen, 2006). Third, the involvement of Rab5 and Rab7A small GTPases in the formation of the prephagosomal vacuole during phagosome maturation is unique to *E. histolytica* (Saito-Nakano *et al.*, 2004; 2007; Nakada-Tsukui *et al.*, 2005). Fourth, phagosome acidification proceeds very rapidly and is completed within 2–5 min (Saito-Nakano *et al.*, 2004; Mitra *et al.*, 2005; 2006). These remarkable differences in the kinetics of phagosome maturation and the diversity of molecules involved in the process strongly suggest that the underlying mechanisms of phagocytosis and phagosomal maturation in this organism may be significantly divergent.

Recently, membrane phospholipids have been shown to play a pivotal role as mediators of membrane trafficking, cytoskeletal re-arrangement and cell surface receptor signalling (Lindmo and Stenmark, 2006). Membrane phosphatidylinositol (PtdIns) metabolism, in particular, has also been implicated in the regulation of phagocytosis (Fratti *et al.*, 2001; Botelho *et al.*, 2004; Scott *et al.*, 2005; Yeung *et al.*, 2006). In addition, phagosome maturation is blocked when phosphatidylinositol-3-phosphate [PtdIns(3)P] generation on the phagosome membrane is inhibited. Under normal conditions, the formation of PtdIns(3)P on the surface of phagosomes subsequently results in the recruitment of PtdIns(3)-P-binding proteins, including early endosome antigen-1 (EEA1) and hepatocyte growth factor-regulated tyrosine kinase substrate (Hrs) (Gillooly *et al.*, 2001; Chua and Deretic, 2004; Vieira *et al.*, 2004). Altogether, these studies indicate that PtdInss are important regulators of phagocytosis and phagosome maturation.

PtdIns(3)P was also implicated in the phagocytosis and endocytosis of *E. histolytica*, in a study where wortmannin, a potent inhibitor for phosphatidylinositol 3-kinase, was used (Ghosh and Samuelson, 1997; Powell *et al.*, 2006). However, *E. histolytica* lacks PtdIns(3)P effectors found in other organisms, including EEA1 and Hrs (Loftus *et al.*, 2005; Clark *et al.*, 2007). To better understand the involvement of lipid mediators in *E. histolytica*, and to uncover the molecular mechanism behind the inhibition of phagocyosis by wortmannin, we investigated the role of PtdIns(3)P and PtdIns-phosphate (PtdIns-P)-binding proteins during phagocytosis in *E. histolytica*. We have chosen to study PtdIns(3)P first because it has been implicated as the major regulator of endosome and phagosome maturation (Botelho *et al.*, 2004; Lindmo and Stenmark, 2006; Yeung *et al.*, 2006), and the specific biomarker for PtdIns(3)P is readily available (Gillooly *et al.*, 2000; Balla, 2005). A genome-wide survey of the *E. histolytica* database has shown that 12 FYVE (Fab-1, YGL023, Vps27, EEA1) domain-containing proteins are present in this organism, 11 of which reveal a unique modular structures consisting of the RhoGEF, pleckstrin homology (PH) and FYVE domains. We demonstrate the unique kinetics of PtdIns(3)P in phagocytosis by time-lapse live monitoring of PtdIns(3)P using a transgenic cell line expressing green fluorescent protein (GFP)-fused with the FYVE domain from Hrs. We subsequently demonstrate that among the 12 *E. histolytica* FYVE-domain-containing proteins (EhFP1-12), EhFP4 is specifically recruited to the phagocytic cup upon internalization of a mammalian cell, and is colocalized with F-actin. We further show that the unexpected phosphoinositide specificity of EhFP4 is mediated by its unique carboxyl terminal region, and that four Rho/Rac small GTPases serve as the downstream effectors of EhFP4.

Results

PtdIns(3)P is localized on the membrane of internal vesicles in the quiescent state, and not primarily in endosomes

We examined the kinetics of PtdIns(3)P, which is known to be involved in endosome and phagosome maturation in other organisms (Gillooly *et al.*, 2001), during endocytosis and phagocytosis in *E. histolytica*. To this end, we generated an *E. histolytica* transformant expressing GFP fused with the FYVE (Fab-1, YGL023, Vps27, EEA1) domain from hepatocyte growth factor 1-regulated tyrosine kinase substrate (Hrs), which has been used in other studies to probe the localization of PtdIns(3)P (Burd and Emr, 1998; Gaullier *et al.*, 1998; Gillooly *et al.*, 2000; Ellson *et al.*, 2001; Balla, 2005; Halet, 2005). The expression of the GFP–Hrs–FYVE fusion protein as a homogeneous 52 kDa protein was confirmed by immunoblot (Fig. 1A). Confocal photomicrographs revealed that the GFP–Hrs–FYVE signal was restricted to the membrane of a limited number of internal vesicles/vacuoles (Fig. 1B, a–c). It was shown that in mammalian cells, PtdIns(3)P is localized to the membrane of early endosomes and to the internal membranes of multivesicular endosomes, suggesting the general involvement of PtdIns(3)P in the endocytic pathway (Gillooly *et al.*, 2000).

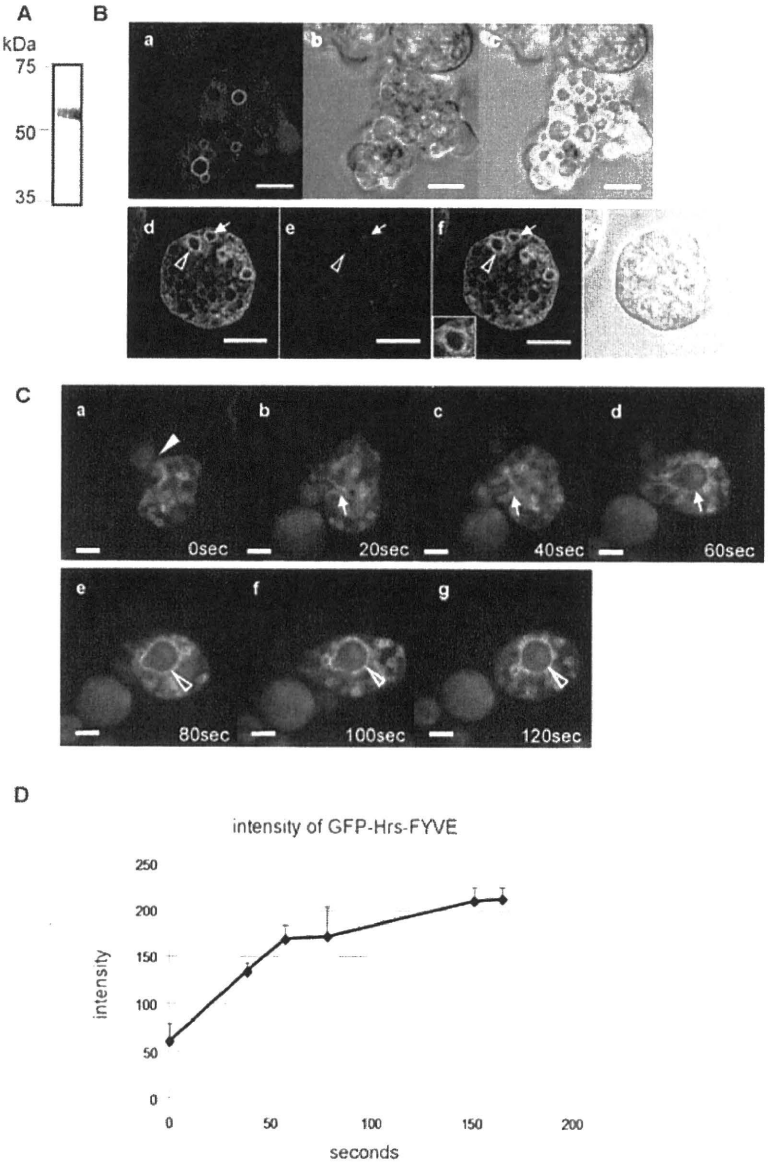

Fig. 1. Expression and localization of GFP–Hrs–FYVE in *E. histolytica*.
A. Immunoblot of the lysate from a *E. histolytica* transformant expressing GFP–Hrs–FYVE. A single 52 kDa band corresponding to myc-GFP–Hrs–FYVE fusion protein was detected by immunoblot analysis using anti-myc antibody.
B. Localization of GFP–Hrs–FYVE in the quiescent stage (a–c) and lack of colocalization of a fluid-phase marker, RITC-dextran (d–g). GFP–Hrs–FYVE-expressing *E. histolytica* trophozoites were fixed and analysed by Zeiss LSM 510. (a–c) GFP–Hrs–FYVE is localized on internal vesicles/vacuoles in the quiescent stage [a, GFP; b, differential interference contrast (DIC); c, merge]. (d–g) GFP–Hrs–FYVE expressing transformants were incubated with 2 mg ml^{-1} RITC-dextran for 10 min, fixed, and examined. (d, GFP; e, RITC-dextran; f, merge; g, DIC). Arrows indicate primary endosomes with PtdIns(3)P, open arrowheads indicate multivesicular bodies or secondary endosomes associated with PtdIns(3)P. A highly magnified image of a representative endosome-containing vacuole (open arrowheads) is shown in an islet (f). Bars, 10 μm.
C. Time-lapse images of localization of GFP–Hrs–FYVE during CHO cell phagocytosis. CHO cells were labelled with Cell tracker blue and added to the GFP–Hrs–FYVE-expressing *E. histolytica* culture (approximately 1:2 ratio). Images were captured by Leica AS-MDW at given times. The exact timing of attachment of CHO cell by *E. histolytica* was manually monitored and defined as time 0. A filled arrowhead marks the attachment point between the *E. histolytica* and a CHO cell. Arrows depict the phagocytic cups and open arrowheads indicate phagosomes containing CHO cells. Bars, 10 μm.
D. The kinetics of GFP–Hrs–FYVE recruitment on the nascent phagosome. The GFP fluorescence of the phagocytic cup and phagosome was measured using the *profile tool* in the Carl Zeiss LSM510. The mean and standard deviation of five random measurements are shown. Representative fluorescence profiles of a phagosome at two time points (0.2 and 164.4 s) are shown in Fig. S1.

To examine the association of PtdIns(3)P in the endocytic pathways in *E. histolytica*, the GFP–Hrs–FYVE-expressing transformant was incubated with 2 mg ml^{-1} RITC-dextran for 5, 10, 30, 60 and 90 min to allow endocytosis to take place. The number of RITC-dextran-containing endosomes associated or not associated with GFP–FYVE was counted, and the percentage of GFP–FYVE positive endosomes was calculated. At each time point, 14.0 ± 15.3%, 7.3 ± 7.9%, 1.4 ± 2.5%, 1.3 ± 0.8% and 2.0 ± 1.4% of the endosomes containing RITC-dextran were found to be associated with PtdIns(3)P respectively (Fig. 1B, d–g). The majority of the PtdIns(3)P-positive vacuoles contained RITC-dextran-positive vesicles in a confined area (Fig. 1B, f, islet), suggestive of multivesicular bodies (Saito-Nakano *et al.*, 2004). These data suggest that PtdIns(3)P is partially associated with endocytosis in the early phase and with multivesicular body formation. The majority of endosomes, however, are not associated with PtdIns(3)P during the steady state in this organism. The specificity of the Hrs–FYVE domain to PtdIns(3)P was verified by the phospholipid binding assay (see below, Fig. 4B, a).

Rapid recruitment of PtdIns(3)P to the phagocytic cup and phagosomes during phagocytosis of CHO cells

To investigate the involvement of PtdIns(3)P signalling in phagocytosis and phagosome maturation, we examined the localization of PtdIns(3)P during the course of engulfment of CHO cells. Cell tracker-loaded CHO cells were mixed with the amoeba transformants and the dynamics of PtdIns(3)P during their interaction and subsequent phagocytosis of CHO cells were monitored by real-time live imaging. We observed two types of phagocytosis based on their kinetics. Two-thirds (64.2 ± 6.8%) of the observed phagocytic events were completed within 3 min ('fast phagocytosis'), while one quarter (26.6 ± 7.3%) required more than 10 min to be completed ('slow phagocytosis') (K. Nakada-Tsukui, unpublished). In both types of phagocytosis, PtdIns(3)P was recruited to the phagocytic cup and phagosomes. The kinetics of PtdIns(3)P during the fast phagocytosis was as follows: less than 20 s after the adherence of the CHO cells, PtdIns(3)P started to accumulate on the phagocytic cup, and upon closure of the phagosome, PtdIns(3)P extended along the entire phagosome membrane (Fig. 1C and Video S1). The kinetics of the recruitment of GFP–Hrs–FYVE on the nascent phagosome was further analysed (Fig. 1D and Fig. S1). A time-dependent linear accumulation of the GFP signal was observed up to 160 s. In 'fast phagocytosis', the entire process from the formation of the phagocytic cup to the closure of the phagosome membrane was completed within 80 s. In this example, PtdIns(3)P remained on the phagosome membrane for at least 1 h after the closure of the phagosome.

In 'slow phagocytosis', instead of internalizing the CHO cell as a whole, *E. histolytica* gradually internalized its content through a narrow tunnel that was generated upon adherence (Video S2). This tunnel-like structure, containing a small portion of CHO cell, often persisted for more than 30 min without closure of the phagocytic cup. During this process, PtdIns(3)P also accumulated on the phagocytic cup right after the internalization, and remained on both the tunnel-like structure and the phagosome membrane. As shown in Videos S1 and S2, thread-like structures were often observed to be associated with GFP–Hrs–FYVE between PtdIns(3)P-positive vacuoles. These PtdIns(3)P-associated thread-like structures were seldom observed during the quiescent stage, suggesting that phagocytosis-induced PtdIns(3)P signalling is likely involved in the formation of these structures.

The 'slow phagocytosis' demonstrated here was also described in earlier studies in *Entamoeba* (Lejeune and Gicquaud, 1987; 1992), and appears to be similar to the PtdIns 3-kinase-dependent constriction of phagosomes described by Swanson *et al.* (1999). This observation may reflect the inability to complete the phagocytic process normally.

We further calculated the percentage of phagosomes associated with PtdIns(3)P during phagocytosis. GFP–Hrs–FYVE expressing amoebas were co-cultured with Cell tracker blue-loaded CHO cells for 10, 30 and 60 min. The phagosomes and phagocytic cups positive for GFP–Hrs–FYVE were counted under a confocal microscope. At 10, 30 and 60 min of cocultivation, 69 ± 6.7%, 51 ± 4.5% and 27 ± 5.7% of phagosomes were associated with PtdIns(3)P while 75% of the phagocytic cups were also PtdIns(3)P positive (Fig. S2). Although we did not distinguish fast and slow phagocytosis in this experiment, PtdIns(3)P association was predominantly observed on the phagosomes at the early time points of phagocytosis and also on the phagocytic cups. These results suggest that phagocytosis predominantly (> 70% of the phagocytosis events) occurs in a PtdIns(3)P-dependent manner.

Expression of GFP–Hrs–FYVE does not affect endocytosis, phagosome acidification and degradation of internalized materials in the phagosomes

To exclude the possibility that expression of GFP–Hrs–FYVE affects the normal kinetics of phagosome maturation, e.g. acidification and degradation of its content, we examined the kinetics of the phagosome pH in the red fluorescent protein (RFP)-Hrs–FYVE-expressing and control RFP-expressing transformants, by the previously described method using FITC-conjugated yeasts (Mitra *et al.*, 2005; 2006; Saito-Nakano *et al.*, 2007). The

kinetics of the phagosomal pH in these transformants was similar to each other (B.N. Mitra, data not shown), and also to that of the wild-type amoeba (Mitra *et al.*, 2005). We also compared the kinetics of degradation of an ingested *Leishmania* promastigote expressing GFP in a phagosome by measuring fluorescence intensity (Mitra *et al.*, 2005; 2006; Saito-Nakano *et al.*, 2007). Similar to the results of the acidification kinetics, the kinetics of GFP decay of ingested *Leishmania* parasites in both transformants was comparable (B.N. Mitra, data not shown). Thus, expression of the Hrs–FYVE domain does not affect phagosome maturation and degradation of endocytosed materials in the phagosomes.

We further examined if endocytosis is affected by GFP–Hrs–FYVE expression. The rate of endocytosis of RITC-dextran was indistinguishable between the GFP and GFP–Hrs–FYVE transformants (K. Nakada-Tsukui, data not shown). Thus, although we were not able to examine colocalization of RITC-dextran and GFP–Hrs–FYVE at the very early time points (less than 5 min) due to technical problems, we are tempted to conclude that PtdIns(3)P is not primarily involved in endocytosis.

Expression of 12 FYVE domain-containing proteins in E. histolytica

To get more insights into the downstream effectors of PtdIns(3)P during phagocytosis, we performed a genome-wide search for FYVE domain-containing proteins in the *E. histolytica* genome database (http://www.tigr.org/tdb/e2k1/eha1/). The FYVE domain derived from Hrs (Komada *et al.*, 1997) was used as a query sequence. Twelve *E. histolytica* proteins showed significant homology (E-value $< 1.1 \times 10^{-3}$), and we named these proteins EhFP1-12: *E. histolytica* FYVE domain-containing proteins 1–12. Eleven EhFP proteins (EhFP1-11) showed a similar overall structure, containing RhoGEF/DH and PH domains at the amino terminus of the FYVE domain (Fig. 2A). This modular structure containing RhoGEF/DH indicates that these FYVE domain proteins likely modulate cytoskeletal re-arrangement downstream of PtdIns(3)P signalling (Rossman *et al.*, 2005). An expanded repertoire of EhFP gene family suggests the importance of PtdIns-P-mediated signalling in this organism.

The levels of transcription of the EhFP genes were examined using DNA microarray. Total RNA from a reference HM-1:IMSS strain was prepared and hybridized to a custom-made *E. histolytica* DNA microarray (Gilchrist *et al.*, 2006; Ehrenkaufer *et al.*, 2007). Transcriptional levels of individual EhFP genes varied. EhFP5, 6, 7 and 10 were highly expressed (> 50% of the level of RNA polymerase II), while EhFP1, 2, 4, 8 and 12 were moderately expressed (between 20% and 50%), and EhFP3, 9 and 11 were poorly expressed (< 20%). EhFP9 protein was previously detected in phagosomes isolated from another clinical isolate (KU33 strain) by proteomic analysis (Okada *et al.*, 2006).

Intracellular localization of EhFPs and the dynamism of EhFP4 during phagocytosis

To understand the role of individual EhFPs in CHO cell phagocytosis, intracellular localization and their kinetics during phagocytosis were examined using transformants expressing HA-tagged EhFP proteins. Epitope-tag plasmid constructs, to express all EhFPs except EhFP9, and their corresponding transformants were successfully produced. We were unable to clone an EhFP9 protein coding region for unknown reasons despite repeated trials. Protein expression of HA-EhFP1, 2, 4 and 5 was confirmed by immunoblots, while expression of HA-EhFP3, 6, 7, 8, 10 and 12 failed (K. Nakada-Tsukui, unpublished). Analysis of EhFP11 was not included in this study because we found this entry in an updated TIGR database after completing all constructions. In the following experiments, we characterized EhFP1, 2, 4 and 5. The analysis of the remaining EhFPs will be described elsewhere.

Immunofluorescence imaging showed that HA-EhFP1, 2, 4 and 5 were localized throughout the cytoplasm in steady state (K. Nakada-Tsukui, unpublished). During CHO cell phagocytosis, localization of HA-EhFP1 and 2 did not change significantly (Fig. 2B). HA-EhFP5 was weakly associated with the phagocytic cup, and did not associate with the phagosome membrane at a later stage (Fig. 2B). On the other hand, HA-EhFP4 was recruited to the phagocytic cup and to a tunnel-like tubular structure, connecting the plasma membrane and the phagosome (Fig. 2C and Fig. S4). This tunnel-like structure was characteristically observed during 'slow phagocytosis.' The distribution of EhFP4 overlapped with that of F-actin, as demonstrated with anti-HA antibody and phallacidin double staining (Fig. 2D), suggesting the possible involvement of EhFP4 in actin re-arrangement.

Small GTPase RacG, p21 activated kinase PAK1, and calcium binding protein EhCaBP1 have been reported to be involved in phagocytosis (Guillen *et al.*, 1998; Labruyere *et al.*, 2003; Jain *et al.*, 2008). Among them, it was previously shown that upon erythrophagocytosis, EhCaBP1 was transiently recruited to the phagocytic cup and was dissociated from it less than one minute of engulfment (Jain *et al.*, 2008). We examined whether EhFP4 colocalizes with EhCaBP1 during CHO cell phagocytosis (Fig. 2E). Upon direct physical interaction with CHO cells, EhFP4 and EhCaBP1 both accumulated at the contact site (Fig. 2E, a–d). During internalization of CHO cells, the localization of EhCaBP1 appeared to be restricted to the proximal peripheral region of the

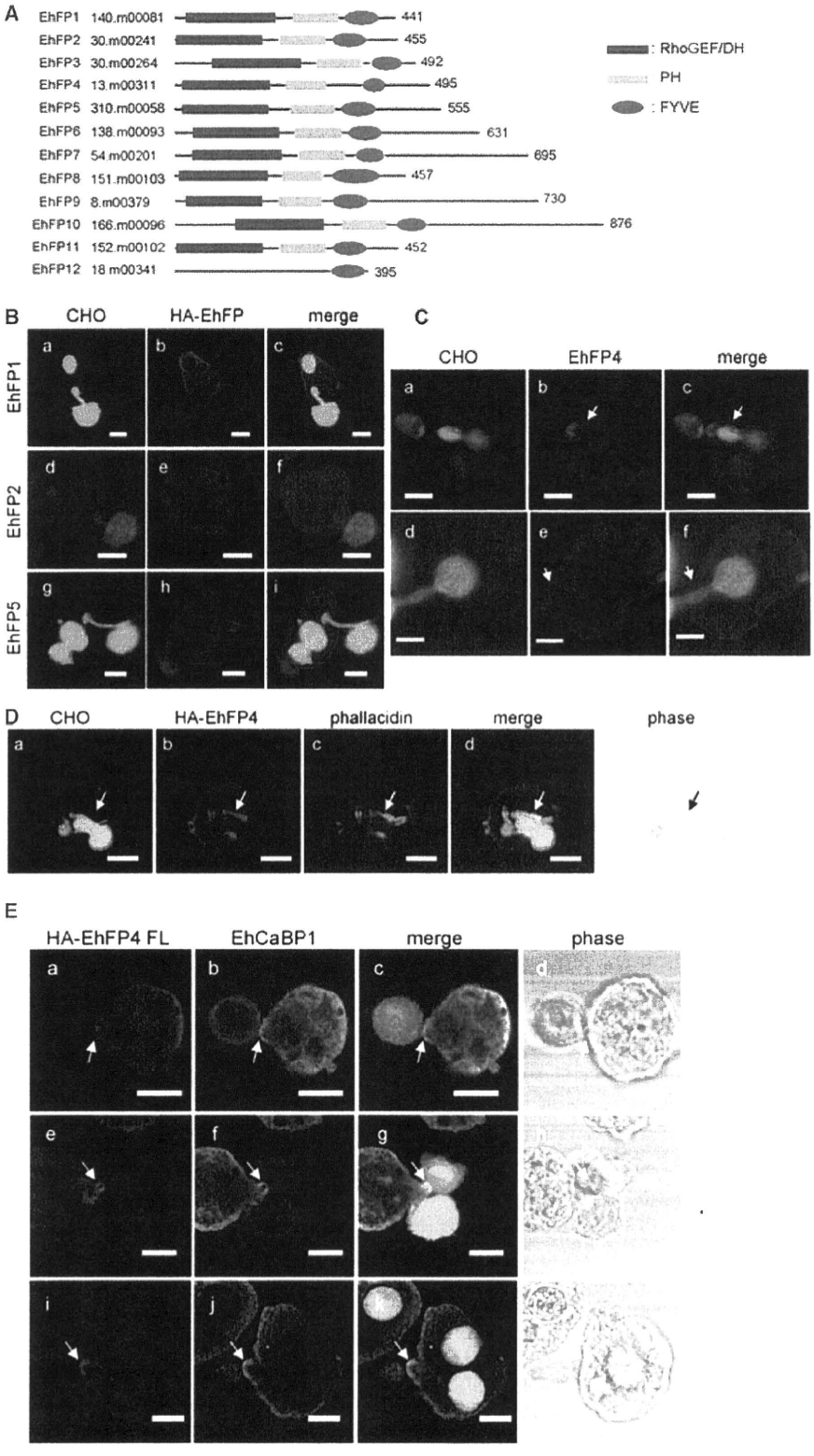
A
EhFP1 140.m00081 441
EhFP2 30.m00241 455
EhFP3 30.m00264 492
EhFP4 13.m00311 495
EhFP5 310.m00058 555
EhFP6 138.m00093 631
EhFP7 54.m00201 695
EhFP8 151.m00103 457
EhFP9 8.m00379 730
EhFP10 166.m00096 876
EhFP11 152.m00102 452
EhFP12 18.m00341 395
: RhoGEF/DH
PH
: FYVE
B
CHO
HA-EhFP
merge
EhFP1
EhFP2
EhFP5
C
CHO
EhFP4
merge
D
CHO
HA-EhFP4
phallacidin
merge
phase
E
HA-EhFP4 FL
EhCaBP1
merge
phase

Fig. 2. FYVE domain-containing proteins in *E. histolytica* (EhFP) and localization of EhFP proteins during CHO cell phagocytosis.
A. A schematic representation of domain structures of EhFP proteins. RhoGEF/DH, pleckstrin homology, or FYVE domains are shown as red, green rectangles or blue ovals respectively. TIGR ID numbers and amino acid numbers of EhFP1–12 are shown.
B and C. Localization of EhFP1, 2, 4 and 5. Trophozoites of the HA-tagged EhFP1-, EhFP2-, EhFP5- (B) or EhFP4-expressing (C) transformants were co-cultured with Cell tracker green-loaded CHO cells for 30 min, fixed and reacted with anti-HA antibody, followed by Alexa-568 conjugated anti-mouse IgG secondary antibody. Bars, 10 μm. Arrows (in C) indicate EhFP4 on the proximal portion of the phagosome (b, c, e and f) and the tunnel-like structures linked to the phagosome (e and f). Bars, 10 μm.
D. Colocalization of EhFP4 and F-actin during CHO cell phagocytosis. HA-EhFP4-expressing trophozoites were co-cultured with Cell tracker blue-loaded CHO cells for 30 min, fixed and reacted with anti-HA and BODIPY FL phallacidin to visualize HA-EhFP4 and F-actin. Arrows indicate EhFP4 and F-actin accumulated at the proximal portion of the phagosome and the tunnel-like structures linked to the phagosome. Bars, 10 μm.
E. Partial colocalization of EhFP4 and EhCaBP1 during CHO cell phagocytosis. HA-EhFP4-expressing *E. histolytica* were co-cultured with Cell tracker blue-loaded CHO cells for 30 min, fixed, and reacted with anti-HA antibody and anti-EhCaBP antibody. The cells were further reacted with Alexa-568 anti-mouse IgG and Alexa-488 anti-rabbit IgG secondary antibody. Arrows indicate regions where HA-EhFP4 and EhCaBP colocalize. Note that Cell tracker blue signal of CHO cells is also seen in the green channel. Bars, 10 μm.

phagocytic cup, while EhFP4 was broadly distributed at the phagocytic cup and the tunnel-like structures (Fig. 2E, e–l).

Localization of EhFP4 to the phagocytic cup is mediated by the FYVE and the carboxyl-terminal (CT) domains

To examine whether the FYVE domain is involved in the EhFP4 recruitment during phagocytosis, a deletion mutant of HA-EhFP4 lacking the FYVE and CT domains, HA-EhFP4DH-PH, was generated. Expression of HA-EhFP4DH-PH protein was confirmed by Western blot analysis as a 40 kDa band and the level of its expression was comparable to that of HA-EhFP4 (K. Nakada-Tsukui, data not shown). The localization of this truncation mutant to the phagocytic cup and the tubular tunnel structure was remarkably reduced (Fig. 3A and Fig. S4). However, the recruitment of HA-EhFP4DH-PH to the phagocytic cup was not totally abolished most likely due to the interaction with other unidentified proteins that localize to the phagocytic cup. Taken together, these data suggest that EhFP4 is localized to the phagocytic cup and the phagosome via the FYVE domain and/or CT domain.

To perform live-imaging of EhFP4, we attempted to create an amoeba transformant expressing GFP full-length EhFP4 (EhFP4FL), but failed. We instead created a transformant expressing two tandem repeats of the FYVE domain of EhFP4 fused with GFP (GFP–EhFP4–FYVE), and examined its localization and dynamism. GFP–EhFP4–FYVE was localized diffusely to the cytoplasm under the quiescent state (Fig. 3B, a and b). During CHO cell phagocytosis, GFP–EhFP4–FYVE was recruited to the phagocytic cup and the tunnel-like structure (Fig. 3B, c–j), in a manner very similar to that of HA-EhFP4 (Figs 2C and 3A, and Fig. S4). This result supports the hypothesis that the FYVE domain mainly defines the localization of EhFP4. However, there is a possibility that domains other than the FYVE domain also have a role to define the localization. To understand the role of these domains of EhFP4 in localization and lipid binding, we next examined the lipid binding specificity.

Phosphoinositide specificity of EhFP4

To examine the specificity of EhFP4 towards various phosphoinositides and phospholipids. Lipid binding assay was performed using GST-fused Hrs-2xFYVE (GST–Hrs–FYVE), GST fusion proteins of EhFP4 FYVE, or CT domains (GST–EhFP4–FYVE or GST–EhFP4–CT respectively), and His tag-trigger factor (TF) fusion proteins of full-length EhFP4 (TF–EhFP4FL), FYVE/CT domain-deleted EhFP4 (TF–EhFP4DH–PH), and RhoGEF/DH domain of EhFP4 (TF–EhFP4DH) (Fig. 4B). As expected, GST–Hrs–FYVE showed specific binding to PtdIns(3)P and TF showed no interaction with phosphoinositides and phospholipids (Fig. 4B, a and b). Surprisingly, TF–EhFP4FL strongly bound to PtdIns(4)P, and weakly to PtdIns(3)P and PtdIns(5)P (Figs 4B, c). This interaction was not observed with TF-EhFP4 DH-PH, suggesting that the interaction occurs via the FYVE and/or CT domain(s) (Fig. 4B, d). Furthermore, neither TF–EhFP4DH nor GST–EhFP4–FYVE showed binding with phosphoinositides and phospholipids (Fig. 4B, e and f). This is in marked contrast with the specific binding of Hrs–FYVE to PtdIns(3)P (Gillooly *et al.*, 2000). The GST–EhFP4–CT protein unexpectedly bound to PtdIns(3)P, PtdIns(4)P and weakly to PtdIns(5)P (Fig. 4B, g). GST–EhFP4PH could not be produced in a soluble form (K. Nakada-Tsukui, unpubl. data).

To further confirm that the FYVE domain is not involved in the interaction of EhFP4 with phospholipids, we created TF-EhFP4 FL recombinant proteins in which one or two residues, shown to be involved in PtdIns(3)P binding or affect endosomal localization of EEA1, were mutated: His365Ser/His366Ser (HS) and Cys375Ser (CS) mutants (Stenmark *et al.*, 1996; 2002). Both the mutants equally bound to PtdIns(3)P, PtdIns(4) and PtdIns(5)P, in a similar fashion to TF–EhFP4FL (Fig. 4B, h and i).

EhFP4FLCS mutant was expressed as an amino-terminal HA fusion protein and its localization was examined by indirect immunofluorescence assay (Fig. 4C). The distribution of EhFP4FLCS mutant was indistinguishable from that of the wild-type. EhFP4FLCS mutant was distributed to the cytosol in steady state (Fig. 4C, a–d), and

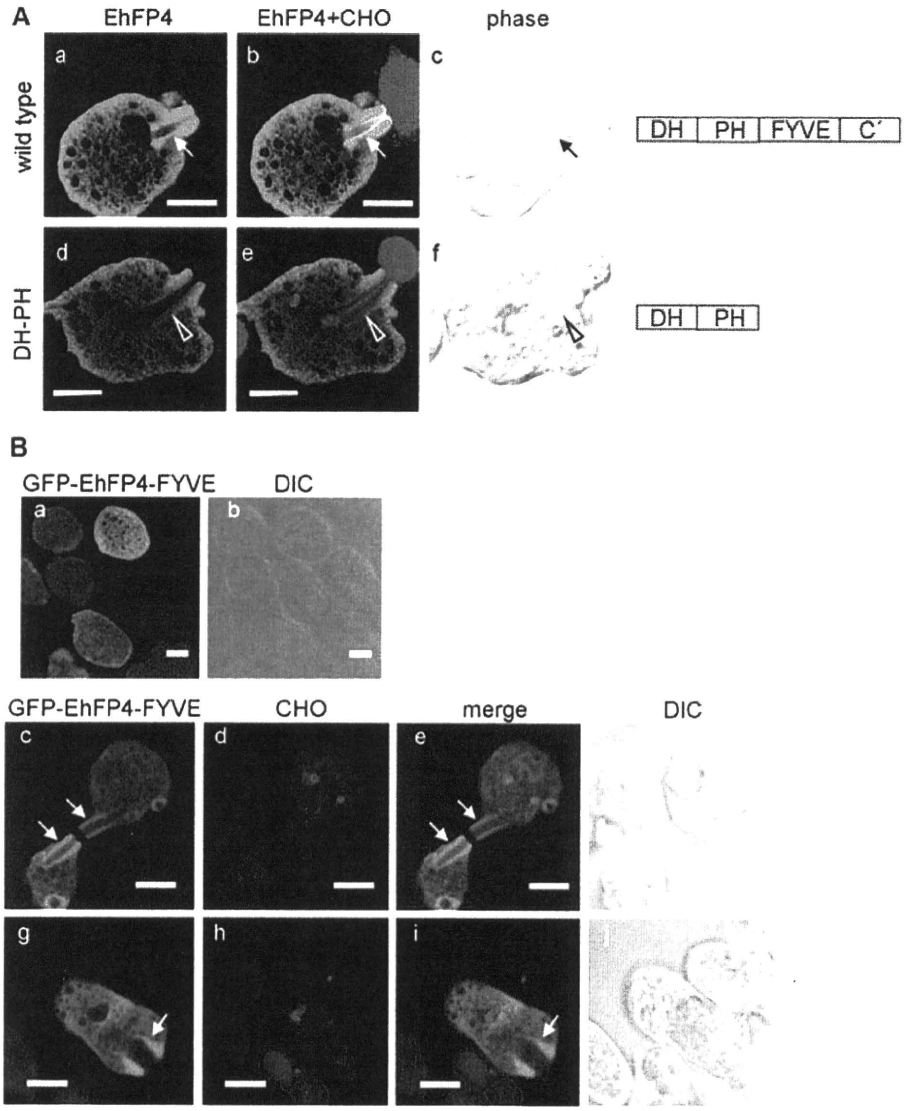

Fig. 3. Involvement of FYVE and CT domains in the EhFP4 recruitment to the phagocytic cup and the tunnel-like structure during phagocytosis.
A. Localization of wild-type EhFP4 (a–c) and mutant EhFP4 lacking FYVE domain ('DH-PH', d–f). Trophozoites of the transformants expressing HA-EhFP4 or HA-EhFP4DH-PH were co-cultured with Cell tracker orange-loaded CHO cells for 30 min, fixed, reacted with anti-HA antibody and Alexa-488 conjugated anti-mouse IgG secondary antibody. Arrows indicate HA-EhFP4 on the tunnel-like structure. Open arrowheads indicate the structures not associated with HA-EhFP4DH-PH. Bars, 10 μm. Three additional trophozoites of wild-type EhFP4 and EhFP4DH-PH are also shown in Fig. S4.
B. Localization of GFP–EhFP4–FYVE in the quiescent state (before phagocytosis, a and b) and during phagocytosis (c–j). Arrows indicate GFP–EhFP4–FYVE on the tunnel-like structure. Bars, 10 μm.

concentrated to the phagocytic cup and the tunnel-like structure (i–p), similar to the wild-type EhFP4 (Fig. 3B), while EhFP4FLCS mutant was not accumulated on phagosomes (Fig. 4C, e–h). Together, these data suggest that the EhFP4 recruitment to the phagocytic cup is mainly regulated by the phospholipid binding via the CT domain, and that the FYVE domain only modulates the specificity of the phospholipid binding of the EhFP4 CT domain.

Identification of Rho/Rac small GTPases as downstream effectors of EhFP4

The close association of EhFP4 with F-actin during phagocytosis, as shown in Fig. 2D, and the presence of the RhoGEF/DH domain in EhFP4 led us to speculate that EhFP4 mediates actin re-arrangement via activation of Rho/Rac small GTPases. Thus, we attempted to identify Rho/Rac proteins that interact with EhFP4. In the

E. histolytica genome database, 24 Rho/Rac genes were identified. Among them 10 highly transcribed Rho/Rac genes were selected based on a transcriptome analysis (Fig. 5A): 108.m00133 (EhRacC; Lohia and Samuelson, 1993), 52.m00167 (EhRho1; Lohia and Samuelson, 1996), 140.m00084, 146.m00106 (EhRacG; Guillen *et al.*, 1998), 16.m00303 (EhRacD; Lohia and Samuelson, 1993), 197.m00080 (EhRacA; Lohia and Samuelson, 1993), 296.m00051, 87.m00159, 46.m00231 and 69.m00185. Detailed analysis of the microarray study will be discussed elsewhere.

We examined physical interaction of TF–EhFP4FL, TF–EhFP4DH–PH or TF with GST-fused Rho/Rac proteins. It was previously shown that RhoGEF/DHs preferentially interact with the nucleotide-free form of Rho/Rac (Rossman *et al.*, 2005). Purified GST-Rho/Rac protein was immobilized with glutathione-Sepharose resin and bound guanine nucleotides were removed by EDTA treatment. The resin was then mixed with TF–EhFP4FL, TF–EhFP4DH–PH or TF. After washing, unbound and bound fractions were analysed by immunoblot analysis with anti-His or anti-GST antibodies (Fig. 5B). Four Rho/Rac molecules, 108.m00133 (EhRacC), 16.m00303 (EhRacD), 87.m00159 and 46.m00231, bound to both TF–EhFP4FL and TF–EhFP4DH–PH, but not with TF. Neither control GST–EhRab7A nor GST bound to TF–EhFP4FL, TF–EhFP4DH–PH or TF. 69.m00185 also showed weak, and inconsistent binding, possibly due to instability of the recombinant protein (K. Nakada-Tsukui, unpublished). We were unable to detect guanine nucleotide (GDP/GTP) exchange activity of TF-EhFP4, TF–EhFP4DH–PH or the TF–EhFP4–DH towards these Rho/Rac proteins, while GEF activity of EhGEF1 towards RacG (Aguilar-Rojas *et al.*, 2005), was detected under the same conditions.

Expression of the FYVE domain of EhFP4 represses phagocytosis of CHO cells and carboxylated beads

To get more insight into the role of FYVE domain of EhFP4 on CHO cell phagocytosis, we further examined whether expression of the FYVE domain of amoebic EhFP4 or mammalian Hrs affects phagocytosis. GFP–EhFP4–FYVE, GFP–Hrs–FYVE and GFP transformants were incubated with CHO cells or carboxylated beads to allow ingestion for 10, 30 and 60 min, and phagocytosis was analysed by flow cytometry. The percentage of amoebae that ingested CHO cells was remarkably affected by expression of GFP–EhFP4–FYVE or GFP–Hrs–FYVE at all time points (Fig. 6, top left). CHO cell phagocytosis was enhanced by 1.8- to 2.7-fold in the GFP–Hrs–FYVE transformant, and repressed by 50–60% in the GFP–EhFP4–FYVE transformant, when compared with the GFP transformant. In contrast, bead phagocytosis was 5–40% reduced by expression of either GFP–Hrs–FYVE or GFP–EhFP4–FYVE (Fig. 6, bottom).

Discussion

Role of PtdIns(3)P in membrane trafficking in E. histolytica

In this study, we demonstrated the localization of PtdIns(3)P in the pathogenic protist *E. histolytica*. During the quiescent state, PtdIns(3)P localizes to internal vesicles/vacuoles, but not primarily in early endosomes (Fig. 1). The minor contribution of PtdIns(3)P to endosome biosynthesis in this protist, which was also previously shown (Powell *et al.*, 2006), is in sharp contrast to mammals and yeasts, where PtdIns(3)P localizes to endosomes and multivesicular endosomes (Gillooly *et al.*, 2000). It has been well established that PtdIns(3)P functions as a mediator for the endosome and phagosome maturation by recruiting PtdIns(3)P binding proteins, i.e. EEA1 and Hrs, in mammals (Gillooly *et al.*, 2001; Chua and Deretic, 2004; Vieira *et al.*, 2004). Based on the available genome information, *E. histolytica* does not have these effectors, which may explain the lack of PtdIns(3)P association with endosomes. However, we cannot exclude the possibility that PtdIns(3)P is localized to the early endosomes only in the very early phase of endocytosis (within 5 min after internalization), and thus play an important, but transient role in endocytosis.

Powell and colleagues previously reported that during erythrophagocytosis PtdIns(3) accumulated on the phagocytic cup and peripheral phagosomes (i.e. phagosomes located close to the plasma membrane), but not on phagosomes located at the centre of the cell using GST–2xFYVE recombinant protein as a bioprobe (Powell *et al.*, 2006). We also observed that GFP–Hrs–FYVE localized to erythrocyte-containing phagosomes (Fig. S5). Since the same two tandem copies of the FYVE domain from human Hrs were used as a PtdIns(3)P biomarker in both the previous and present studies, the subtle discrepancy of the FYVE localization is most likely due to experimental differences for visualization of PtdIns(3)P. Fixed trophozoites were previously used to detect PtdIns(3)P reacted with GST–2xFYVE (Powell *et al.*, 2006), while we determined the location of PtdIns(3)P using live cells expressing GFP–Hrs–FYVE.

Possible mechanisms of PtdIns(3)P recruitment to the phagosome membrane

We demonstrated by time-lapse live imaging (Videos S1 and S2, and Fig. 1) that PtdIns(3)P was recruited to the newly formed phagosome right after ingestion and accumulated on the phagosome membrane. Ellson *et al.*

A

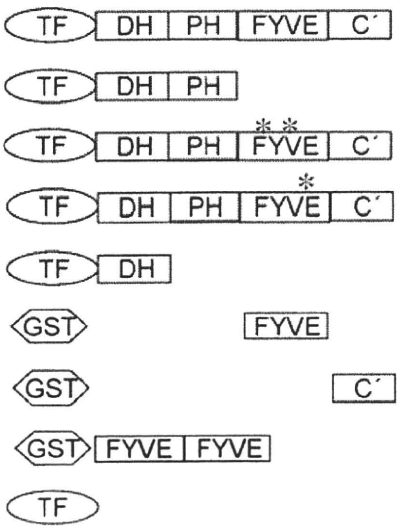

	phospholipid binding
EhFP4 FL	PtdIns(4)P
EhFL4 DH-PH	(-)
EhFP4 FL HS mut	PtdIns(3)P, PtdIns(4)P, PtdIns(5)P
EhFP4 FL CS mut	PtdIns(3)P, PtdIns(4)P, PtdIns(5)P
EhFP4 DH	(-)
EhFP4 FYVE	(-)
EHFP4 CT	PtdIns(3)P, PtdIns(4)P, PtdIns(5)P
Hrs-FYVE	PtdIns(3)P
TF	(-)

B

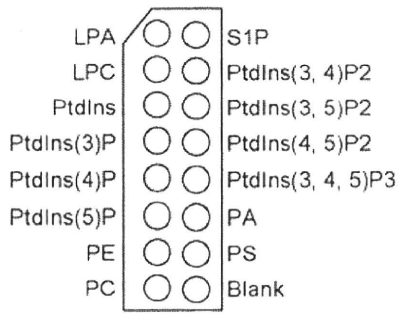

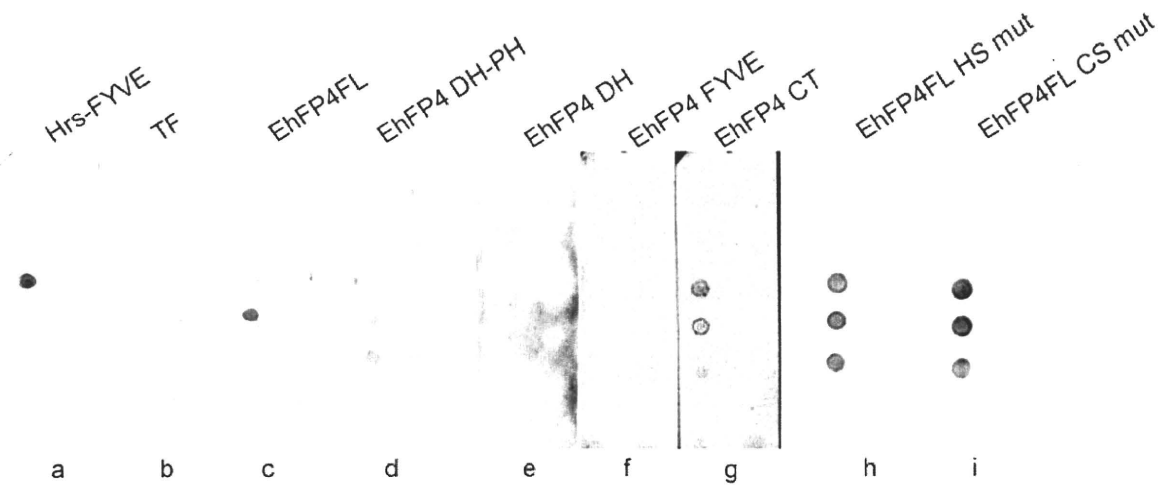

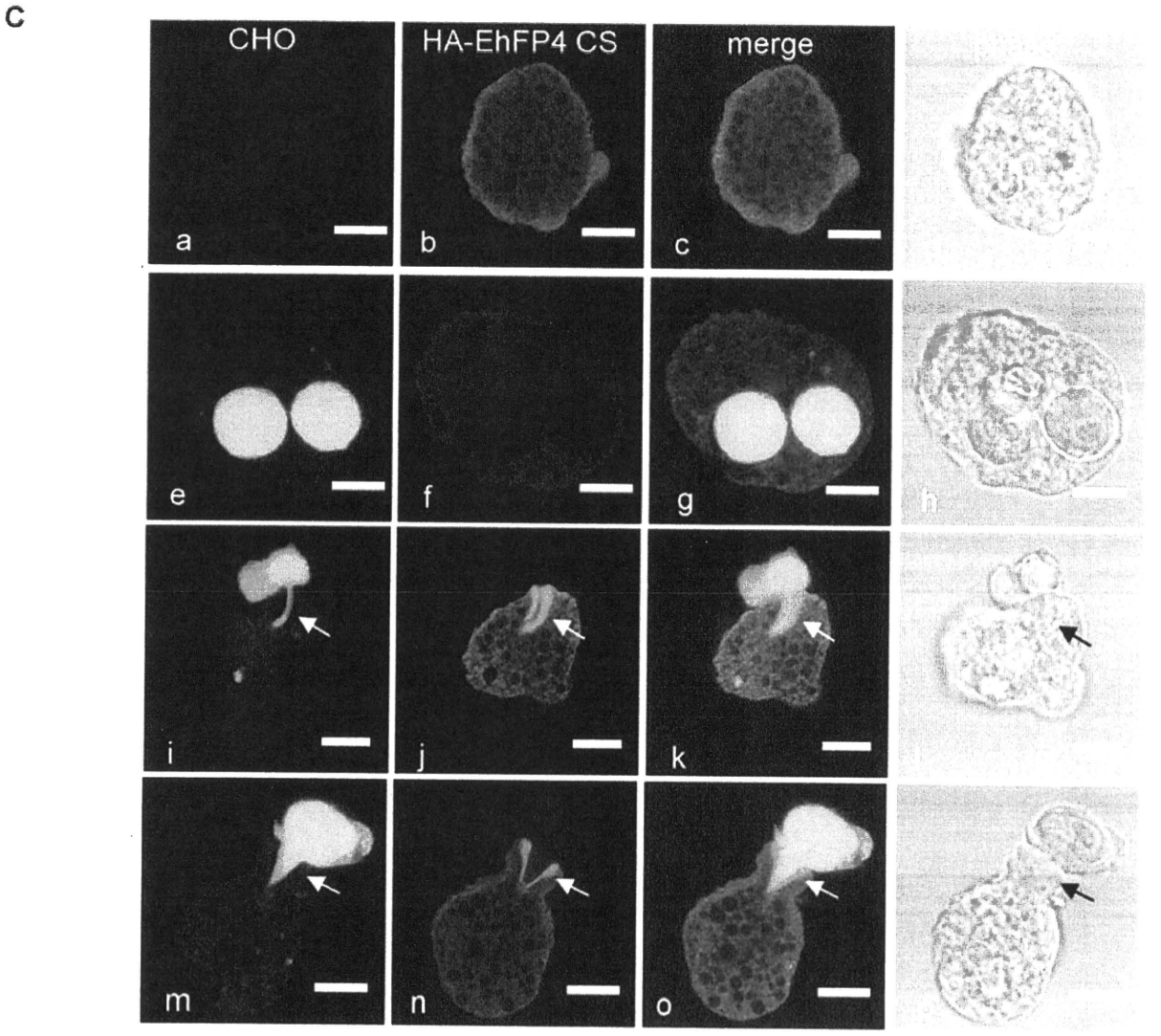

Fig. 4. Phospholipid specificity of EhFP4FL.
A. The domain structures and fusion partners of all the recombinant proteins used in the phospholipid binding study and their phospholipid specificities.
B. Phospholipid specificity of various recombinant proteins corresponding to the full-length or different domains of EhFP4. A GST fusion protein of Hrs–FYVE (GST–Hrs–FYVE) and a TF fusion protein of a full-length EhFP4 (TF–EhFP4FL), a TF fusion protein of EhFP4–DH domain (TF–EhFP4–DH), a GST fusion protein of Eh-FYVE domain or the C-terminal region (GST–EhFP4–FYVE, GST–EhFP4–CT), and two EhFP4 FL variants with a single (Cys375Ser) mutation or double (His365Ser/His366Ser) mutations in the FYVE domain were examined for their binding to various phospholipids. TF was used as a control. Abbreviations are: LPA, lysophosphatidic acid; LPC, lysophosphocholine; PtdIns, phosphatidylinositol; PtdIns(3)P, phosphatidylinositol-3-phosphate; PtdIns(4)P, phosphatidylinositol-4-phosphate; PtdIns(5)P, phosphatidylinositol-5-phosphate; PE, phosphatidylethanolamine; PC, phosphatidylcholine; S1P, sphingosine-1-phosphate; PA, phosphatidic acid; PS, phosphatidylserine.
C. Localization of EhFP4FL Cys375Ser mutant during phagocytosis. The trophozoites expressing HA-tagged EhFP4FL with the Cys375Ser mutation (HA–EhFP4FLCS) were co-cultured with Cell tracker blue-loaded CHO cells for 30 min, fixed and incubated with anti-HA and Alexa-488 conjugated antibody. The cells were then reacted with anti-mouse IgG antibody. (a–d) steady state; (e–h) phagosomes; (i–p) the phagocytic cup and the tunnel-like structure. Arrows indicate the HA–EhFP4FLCS-associated phagocytic cup. Bars, 10 μm.

(2001) reported that PtdIns(3)P is recruited to the phagosomal membrane by *de novo* synthesis of PtdIns(3)P on the phagosome membrane, direct fusion and 'kiss and run' of the PtdIns(3)P-associated vesicles. Our results support that the 'kiss and run' mode of the PtdIns(3)P recruitment is dominant particularly in 'fast phagocytosis'. As shown in Fig. 1C (20 and 40 s, in particular), it was frequently observed that PtdIns(3)P vesicles were

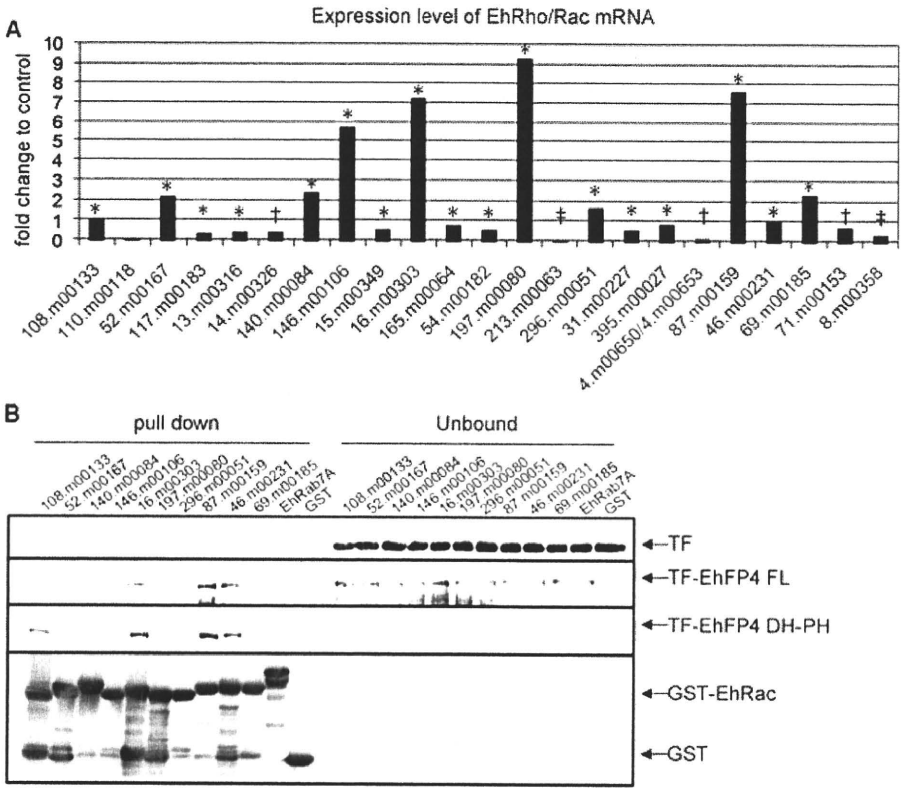

Fig. 5. Expression of *E. histolytica* Rho/Rac small GTPase genes and *in vitro* binding of EhFP4 to recombinant Rho/Rac.
A. The relative mRNA levels of putative Rho/Rac genes to RNA polymerase II is shown, based on a transcriptome analysis using DNA microarray. Detection *P*-value: $^{*}P < 0.00022$, $^{\dagger}P < 0.001$, $^{\ddagger}P < 0.01$.
B. Specific binding of EhFP4 to limited members of Rho/Rac. Glutathione-Sepharose resin bound to 1 of 10 GST–Rho/Rac, GST–Rab7A, or GST was incubated with TF–EhFP4FL, TF–EhFP4DH–PH or TF. After the unbound ('unbound') protein was collected, the resin was extensively washed, and the bound proteins were dissociated from the resin by incubating the resin with SDS-PAGE sample buffer ('pull down'). The 'unbound' and 'pull down' fractions were subjected to SDS-PAGE and immunoblot with anti-His (top three panels) or anti-GST antibody (bottom).

concentrated, accumulated around, and most of them were associated with the phagosome without fusing with the phagocytic cup and phagosome. It was also notable that a dramatic increase in the GFP–Hrs–FYVE signal occurred (Video S1, 1.483 min) soon after the primary phagosome came in contact with another preformed PtdIns(3)P-associated phagosome (0.824 min), but without direct fusion. These observations are consistent with the 'kiss and run' model. However, we could not exclude the possibility that the direct fusion of GFP–Hrs–FYVE-positive vesicles to phagosomes was underestimated because the direct fusion may have occurred too fast to be detected with the imaging system used in the present study. Furthermore, EhVps34, a type III phosphatidylinositol 3-kinase, was detected in phagosomes by proteomics studies (Marion *et al.*, 2005; Okada *et al.*, 2006). Thus, it is conceivable that synthesis of PtdIns(3)P by Vps34 on the phagosomal membrane could also be a source of PtdIns(3)P.

Significance of the intervesicle PtdIns(3)P-associated thread-like structures

We occasionally observed that PtdIns(3)P-associated phagosomes were continuously connected with other GFP–Hrs–FYVE-associated vesicles/vacuoles via the thread-like structures. These thread-like structures may mediate a bulk transfer of PtdIns(3)P from large PtdIns(3)P-positive vacuoles. Since these PtdIns(3)P-associated thread-like structures were often found to connect 'primary' and 'secondary' phagosomes (e.g. Video S2, 3.0 and 3.5 min), they may also serve to efficiently transport membrane and luminal materials necessary for the degradation of the content. Since these PtdIns(3)P-associated thread-like structures were rarely observed in the quiescent stage, their emergence is linked to the activation of PtdIns signalling associated with phagocytosis. Similar structures were reported in mammalian macrophages and *Caenorhabditis elegans* phagocytes (Ellson

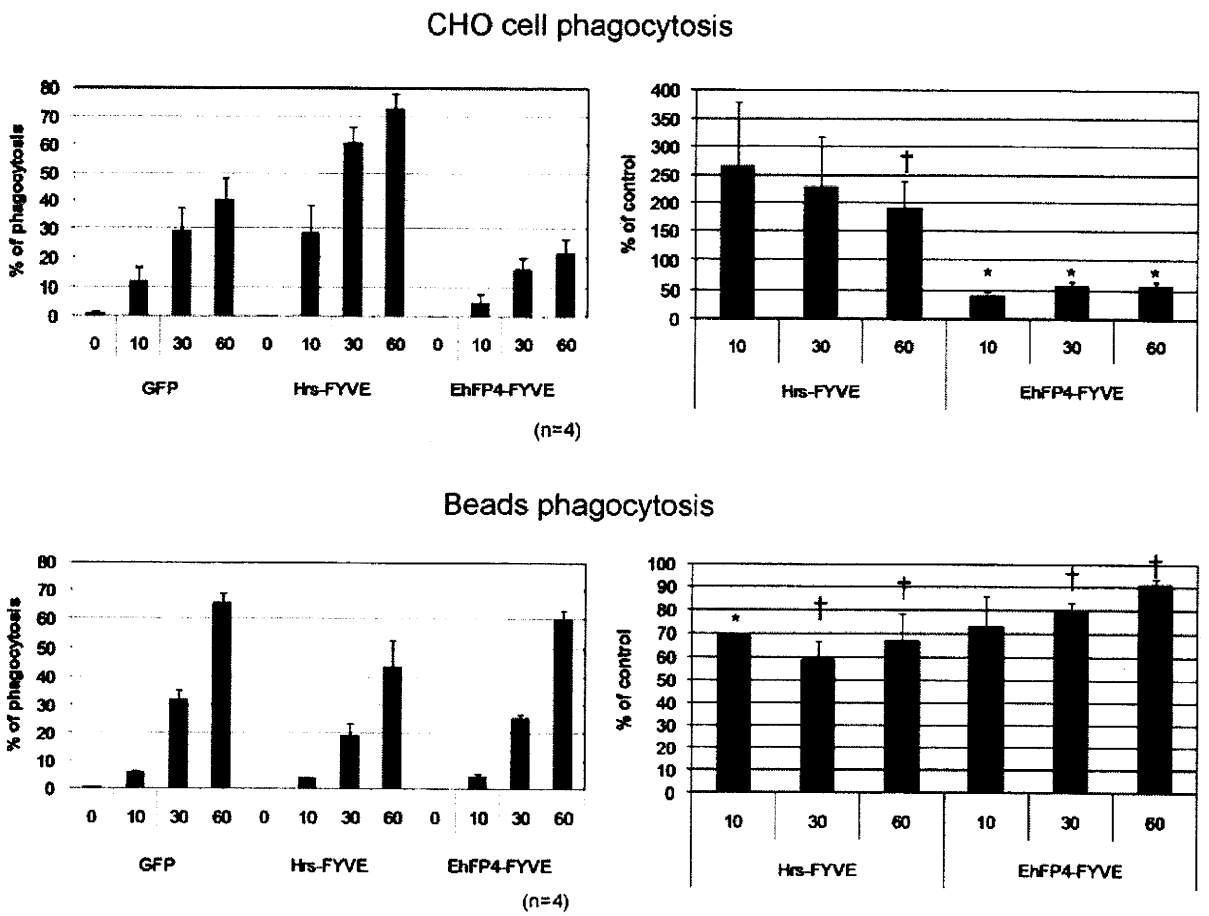

Fig. 6. Effects of Hrs–FYVE and EhFP4-FYVE overexpression on phagocytosis of CHO cells and carboxylated beads. GFP–Hrs–FYVE, GFP–EhFP4–FYVE and GFP transformants were mixed with either CHO cells (top panels) or carboxylated beads (bottom panels) for 0, 10, 30 and 60 min, and the percentage of cells that ingested cells or beads at each time point was calculated (left panels). The percentage of cells that ingested CHO cells or beads in GFP–Hrs–FYVE and GFP–EhFP4–FYVE transformants was also normalized against that of the control GFP transformant and shown in percentage (right panels). The mean and standard deviation of four independent experiments are shown. Asterisks or crosses indicate statistical significance at $P < 0.01$ or $P < 0.05$ respectively, by Student's *t*-test.

et al., 2001; Yu *et al.*, 2008). Interestingly, in *C. elegans*, Rab7, but not PtdIns(3)P, was shown to localize to the structure. These data suggest that interorganelle trafficking via the thread-like structure may be conserved among various organisms, but its components may vary.

Unique expansion of the FYVE-domain-containing protein family in E. histolytica

Entamoeba histolytica possesses a unique set of FYVE domain-containing proteins. Eleven out of 12 EhFP proteins have an identical modular structure consisting of RhoGEF/DH, PH and FYVE domains. Man possesses at least 27 FYVE domain-containing proteins, categorized into 14 groups (Stenmark *et al.*, 2002). A search of the NCBI non-redundant database revealed that 38 proteins possess this particular modular structure: 11 from *E. histolytica* and 27 from other organisms including 5 from *H. sapiens* and 4 from *D. discoideum*. Thus, although this modular structure is conserved in a wide range of organisms from fungi and protists to mammals, the expansion of this protein family in *E. histolytica* is striking and may reflect the reliance and complexity of PtdIns-mediated cellular signalling and network in *E. histolytica*.

A putative homologue of the amoebic RhoGEF-containing EhFPs in mammals may be FGD1, a genetic defect of which was shown to be responsible for faciogenital dysplasia (FGDY). FGD1, consisting of proline-rich, RhoGEF/DH, two PH and FYVE domains (Pasteris *et al.*, 1994), localizes to the Golgi apparatus and the cytoplasm and possesses GEF activity towards Cdc42 (Estrada *et al.*, 2001). The localization of FDG3 mutants lacking individual domains (Pasteris *et al.*, 2000) was unchanged, suggesting that the localization of FDG is

determined by an unidentified domain or redundant domain interactions. In addition, all known mutations of FGD1 in clinical cases of FGDY reside in the RhoGEF/DH or PH domain (Orrico *et al.*, 2000), suggesting the importance of these domains for intracellular targeting and/or activity of FGD1. Recently, dual targeting of FGD2 to early endosomes and membrane ruffles was reported. The FYVE domain was necessary for the targeting of FGD2 to early endosomes (Huber *et al.*, 2008). These data reinforce the importance of the FYVE domain for the recruitment of various proteins via the interaction with PtdIns(3)P. While direct binding of FGD2-FYVE with PtdIns(3)P was not demonstrated, full-length FGD2 recombinant protein was shown to bind to PtdIns(5)P, PtdIns(4,5)P2, PtdIns(3,4,5)P3 and very weakly to PtdIns(3)P. FGD2 FYVE domain was shown to determine the localization of RhoGEF/DH.

Phospholipid specificity of EhFP4 explains distinct localization of Hrs–FYVE and EhFP4 on the phagosome

Although both GFP–Hrs–FYVE and EhFP4 are recruited to the phagosome and the phagosome-associated thread-like structure during phagocytosis, their precise localizations and kinetics of recruitment differed. GFP–Hrs–FYVE was recruited to the entire membrane of phagosomes indiscriminately, while HA-EhFP4 and GFP–EhFP4–FYVE were restricted to the proximal portion of phagosomes and the tunnel-like structure. Phospholipid binding assay revealed that EhFP4 preferentially bound to PtdIns(4)P (Fig. 4B). This finding nicely explains the differential localization and kinetics of GFP–Hrs–FYVE and HA-EhFP4/GFP–EhFP4–FYVE. EhFP4 may be excluded from the distal portion of phagosomes due to the presence of other EhFP protein(s) with affinity to PtdIns(3)P on the phagosome. It is also possible that EhFP4 interacts with unidentified upstream and downstream effectors, which affect its localization.

Furthermore, we showed that the interaction of EhFP4 with PtdIns(3)P, PtdIns(4)P and PtdIns(5)P was not primarily mediated by the FYVE domain, but dependent on the previously unknown CT region (Fig. 4B). The finding that EhFP4-FYVE is not primarily involved in the phospholipid binding was unexpected because all amino acid residues shown to be critical for the PtdIns(3)P binding of EEA1 (Stenmark *et al.*, 2002) are totally conserved in the EhFP4 FYVE domain and GFP–EhFP4–FYVE showed an indistinguishable localization from HA-EhFP4FL. One may argue that dimerization of the FYVE domain is required for the PtdIns(3)P binding (Stenmark *et al.*, 2002). However, the GST fusion protein containing two tandem copies of the FYVE domains of EhFP4, which was expressed in a good yield as a soluble form, also failed to bind PtdIns(3)P, while Hrs–FYVE showed robust PtdIns(3)P-specific binding in the same context (Nakada-Tsukui, unpubl. data and Fig. 4B).

We further showed that the mutations of two conserved amino acids of the FYVE domain altered the phospholipid specificities and enhanced the binding of EhFP4 to PtdIns(3)P and PtdIns(5). Altogether, the EhFP4 FYVE domain likely modulates the phospholipid binding specificity of EhFP4 by either changing the structure of the CT domain or recruiting other protein(s). It remains unexplained how GFP–EhFP4–FYVE, which does not directly bind to phospholipids, localizes to the phagocytic cup, but it is possible that it may be recruited by binding with the endogenous EhFP4 (maybe by binding to the CT domain) or by interacting with other molecules that define its recruitment to the phagocytic cup. In both cases, the dominant negative effect of the GFP–EhFP4–FYVE expression on CHO cell phagocytosis (Fig. 6) may be due to the competition of endogenous EhFP4 or its binding partner(s) that define the localization of endogenous EhFP4 with overxpressed GFP–EhFP4–FYVE. This model needs to be tested in the future.

Specific involvement of EhFP4 and its downstream effectors in phagocytosis

Among four EhFPs examined in the present study, only EhFP4, but not EhFP1, EhFP2 or EhFP5, was involved in phagocytosis *per se*. Since EhFP2, 9 and 10 were previously detected in the phagosome proteome (Marion *et al.*, 2005; Okada *et al.*, 2006), HA-EhFP2 was expected to be associated with phagosomes. EhFP2 was detected in the phagosome proteome with 2.8 μm latex beads coated with human serum (Marion *et al.*, 2005). Therefore, the recruitment of EhFP2 may be dependent on a ligand on the ingested materials. As shown in the present study, the kinetics and morphology of CHO cell phagocytosis is clearly different from bead internalization. As we did not further examine the localization of endogenous EhFP1, 2 and 5 with native antibodies, we were unable to rule out the possibility that the recruitment of these proteins may be perturbed by the amino-terminal HA-tag.

Although we were unable to show RhoGEF activity of recombinant EhFP4, which is often difficult to demonstrate with recombinant protein in other systems also (Crespo *et al.*, 1997), specific interaction of recombinant EhFP4 with EhRacC, EhRacD, 87.m00159, and 46.m00231 has been demonstrated (Fig. 5B). Our failure to demonstrate RhoGEF activity of recombinant EhFP4 may due to lack of post-translational modifications, e.g. phosphorylation as demonstrated to be important in other organisms (Crespo *et al.*, 1997; Schuebel *et al.*, 1998; Suzuki *et al.*, 2003). We have also shown the colocalization of EhFP4 and F-actin (Fig. 2D). Taken together, these results are consistent with the premise that EhFP4 is likely